Electronic and bonding analysis of hardness in pyrite-type transition-metal per-nitrides MN_2

A first-principles investigation

Z. T. Y. Liu[1] S. V. Khare[1], D. Gall[2]

Sanjay V. Khare

Sanjay.khare@utoledo.edu

http://astro1.panet.utoledo.edu/~khare/index.html

[1] Department of Physics and Astronomy
University of Toledo

[2] Department of Materials Science and Engineering
Rensselaer Polytechnic Institute

Motivation for Transition Metal Nitrides (TMNs)

Materials applications interest

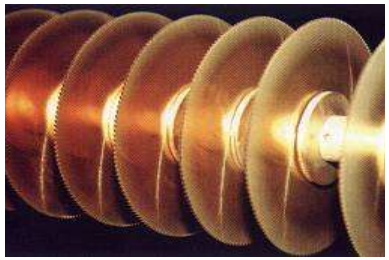

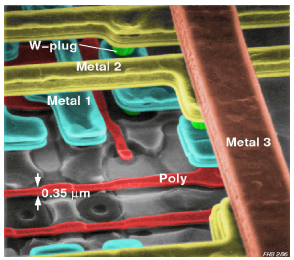

hard coatings optics micro-electronics

Refractory hard materials

Extremely high hardness – wear resistance

High melting points – thermal resistance

Good electrical and thermal conductivity

Good corrosion or oxidation resistance

Elements of Interest

Can we obtain a predictive understanding of intrinsic hardness from first principles computations to guide experiments?

Transition metal elements

	1 H 1.00794																	2 He 4.002602
	3 Li 6.941	4 Be 9.012182											5 B 10.811	C 12.0107	7 N 14.00674	8 O 15.9994	9 F 18.9984032	10 Ne 20.1797
	11 Na 22.989770	12 Mg 24.3050											13 Al 26.581538	14 Si 28.0855	15 P 30.973761	16 S 32.066	17 Cl 35.4527	18 Ar 39.948
3d	19 K 39.0983	20 Ca 40.078	21 Sc 44.955910	22 Ti 47.867	23 V 50.9415	24 Cr 51.9961	25 Mn 54.938049	26 Fe 55.845	27 Co 58.933200	28 Ni 58.6534	29 Cu 63.545	30 Zn 65.39	31 Ga 69.723	32 Ge 72.61	33 As 74.92160	34 Se 78.96	35 Br 79.504	36 Kr 83.80
4d	37 Rb 85.4678	38 Sr 87.62	39 Y 88.90585	40 Zr 91.224	41 Nb 92.90638	42 Mo 95.94	43 Tc (98)	44 Ru 101.07	45 Rh 102.90550	46 Pd 106.42	47 Ag 196.56655	48 Cd 112.411	49 In 114.818	50 Sn 118.710	51 Sb 121.760	52 Te 127.60	53 I 126.90447	54 Xe 131.29
5d	55 Cs 132.90545	56 Ba 137.327	57 La 138.9055	72 Hf 178.49	73 Ta 180.94.79	74 W 183.84	75 Re 186.207	76 Os 190.23	77 Ir 192.217	78 Pt 195.078	79 Au 196.56655	80 Hg 200.59	81 Tl 204.3833	82 Pb 207.2	83 Bi 208.58038	84 Po (209)	85 At (210)	86 Rn (222)
	87 Fr (223)	88 Ra (226)	89 Ac (227)	104 Rf (261)	105 Db (262)	106 Sg (263)	107 Bh (262)	108 Hs (265)	109 Mt (266)	110 (269)	111 (272)	112 (277)		114 (289) (287)		116 (289)		118 (293)

58 Ce 140.116	59 Pr 140.50765	60 Nd 144.24	61 Pm (145)	62 Sm 150.36	63 Eu 151.964	64 Gd 157.25	65 Tb 158.92534	66 Dy 162.50	67 Ho 164.93032	68 Er 167.26	69 Tm 168.93421	70 Yb 173.04	71 Lu 174.967
90 Th 232.0381	91 Pa 231.035888	92 U 238.0289	93 Np (237)	94 Pu (244)	95 Am (243)	96 Cm (247)	97 Bk (247)	98 Cf (251)	99 Es (252)	100 Fm (257)	101 Md (258)	102 No (259)	103 Lr (262)

Published work

Z. T. Y. Liu, D. Gall, and S. V. Khare, Phys. Rev. B **90**, 134102 (2014).

Z. T. Y. Liu, X. Zhou, D. Gall, and S. V. Khare, Comput. Mater. Sci. **84**, 365 (2014).

Z. T. Y. Liu, X. Zhou, S. V. Khare, and D. Gall, J. Phys.-Condens. Matter **26**, 025404 (2014).

X. Zhou, D. Gall and S. V. Khare Journal of Alloys and Compounds **595**, 80 (2014).

S. K. R. Patil, N. S. Mangale, S. V. Khare, and S. Marsillac, Thin Solid Films **517**, 824 (2008).

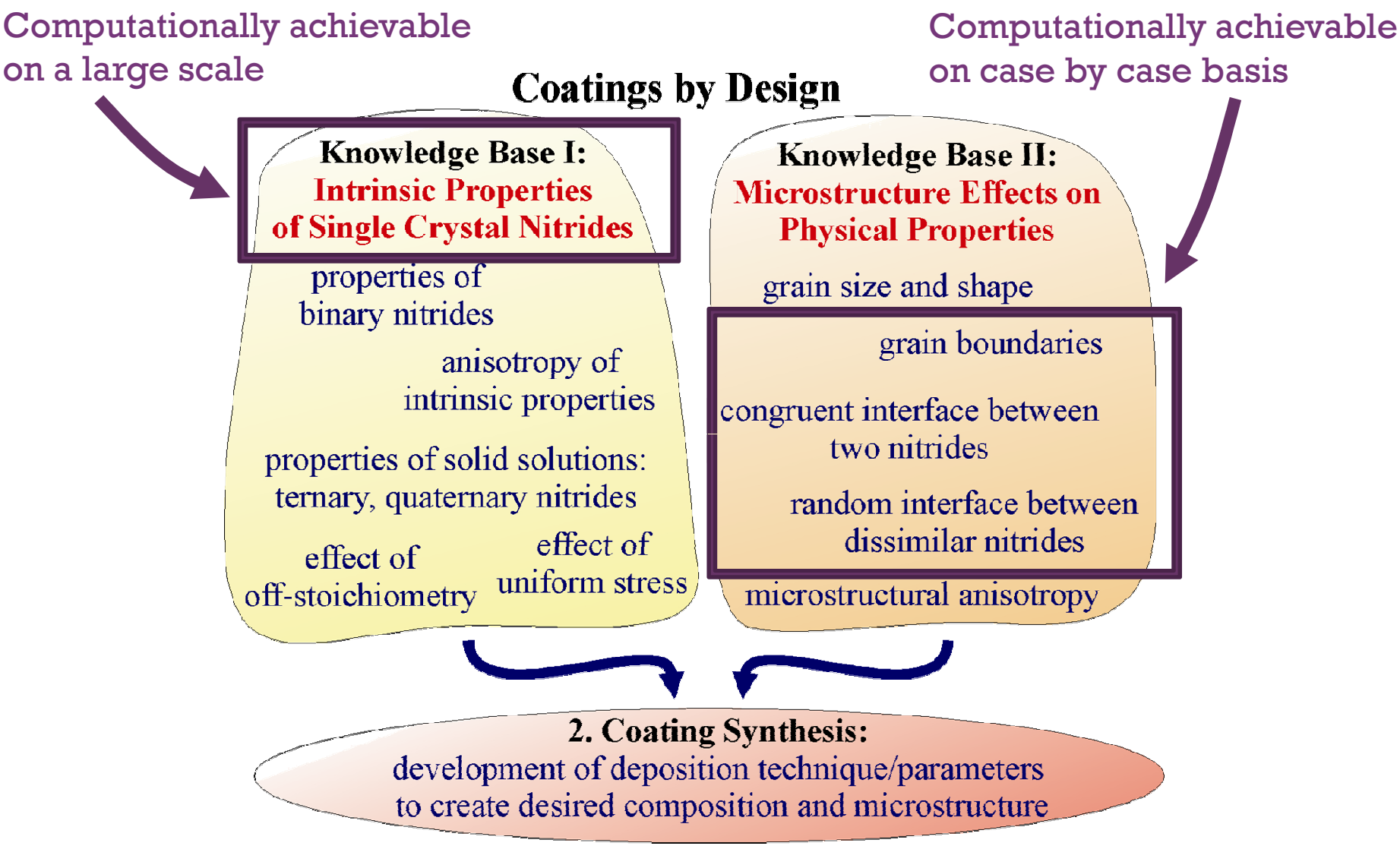
Computationally achievable on a large scale
Computationally achievable on case by case basis
Coatings by Design
Knowledge Base I:
Intrinsic Properties of Single Crystal Nitrides
properties of binary nitrides
anisotropy of intrinsic properties
properties of solid solutions: ternary, quaternary nitrides
effect of off-stoichiometry
effect of uniform stress
Knowledge Base II:
Microstructure Effects on Physical Properties
grain size and shape
grain boundaries
congruent interface between two nitrides
random interface between dissimilar nitrides
microstructural anisotropy
2. Coating Synthesis:
development of deposition technique/parameters to create desired composition and microstructure

Computational Property Database of Likely Cubic Transition Metal Nitrides

M – transition metal

Structures	**Formula**	**Stoichiometry**	3d	4d	5d
M_4N	M_4N	4:1			
Anti-ReO3	M_3N	3:1			
Zinc blende	MN	1:1			
Rocksalt	MN	1:1			
Cesium chloride	MN	1:1			
NbO	MN	1:1			
Th_3P_4	M_3N_4	3:4			
Fluorite	MN_2	0.5:1			
Pyrite	MN_2	0.5:1			

Our published work	About to publish

Materials Genome Initiative (MGI)

Designing Materials to Revolutionize and Engineer our Future (DMREF)

X. Zhou, D. Gall and S. V. Khare, J. Alloys Compd. **80**, 595 (2014).
Z. T. Y. Liu, X. Zhou, S. V. Khare, and D. Gall, J. Phys.-Condens. Matter **26**, 025404 (2014).
Z. T. Y. Liu, X. Zhou, D. Gall, and S. V. Khare, Comput. Mater. Sci. **84**, 365 (2014).
Z. T. Y. Liu, D. Gall, and S. V. Khare, Phys. Rev. B **90**, 134102 (2014).
S. K. R. Patil, N. S. Mangale, S. V. Khare, and S. Marsillac, Thin Solid Films **517**, 824 (2008).

Computed Structures of Transition Metal Nitrides

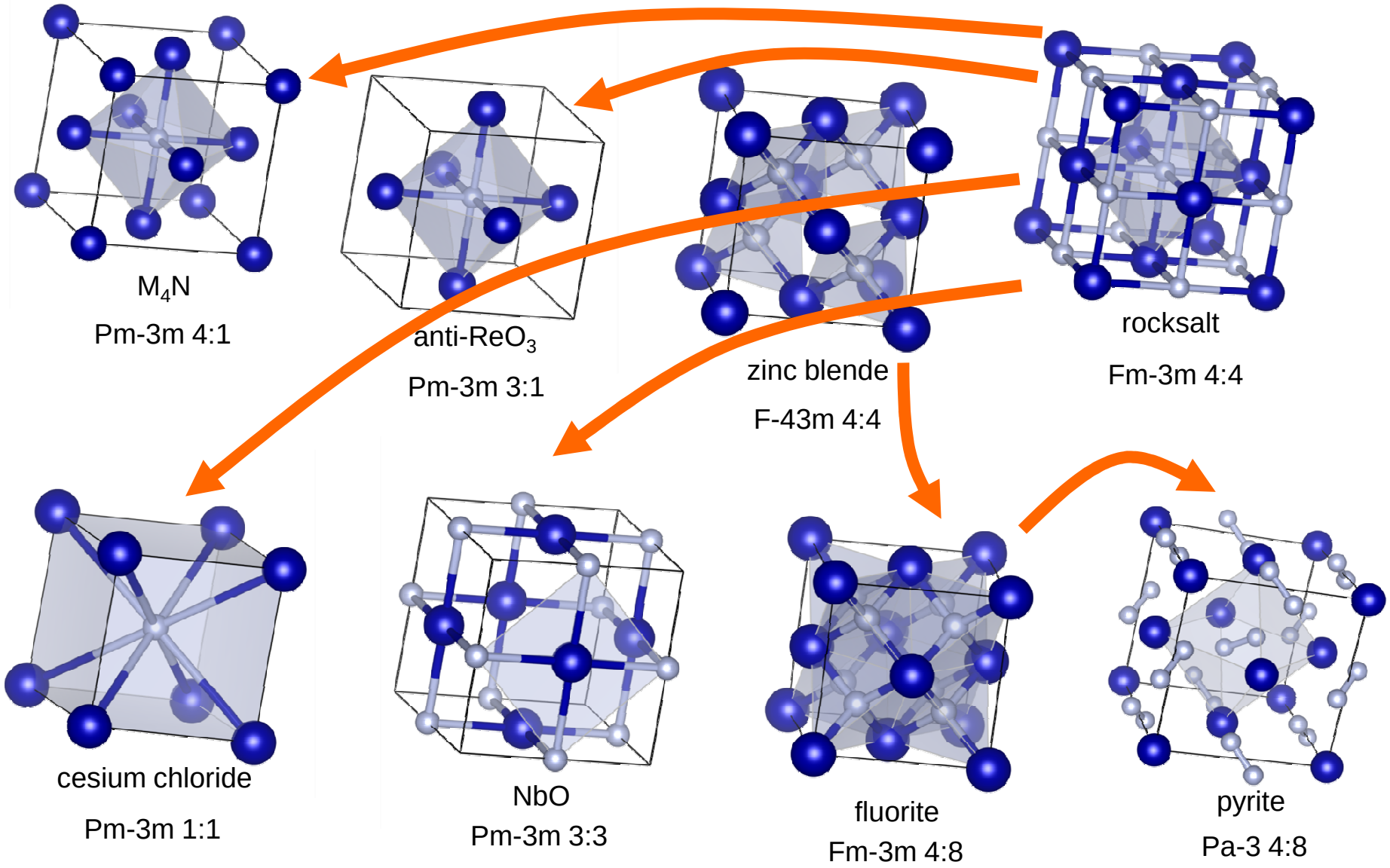

The General Procedure

Choice of compositions and structures

DFT program

Obtain single-crystalline properties
e.g. lattice constant, elastic constants, etc.

effective medium theory

Obtain **averaged** poly-crystalline properties
e.g. mechanical moduli, ratios, hardness

visualization

Visualization

Discover trends and correlations between trends

Identify promising transition metal nitrides and eliminate unfavorable ones

Experimental synthesis of pyrite-type PtN_2

E.Gregoryanz, C. Sanloup, M. Somayazulu, J. Badro, G. Giquet, H-K. Mao, and R. J. Hemley, Nat. Mat. 3, 294 (2004).

Although numerous metals react with nitrogen there are no known binary nitrides of the noble metals. We report the discovery and characterization of platinum nitride (PtN_2), the first binary nitride of the noble metals group.

This compound can be formed above 45–50 GPa and temperatures exceeding 2,000 K, and is stable after quenching to room pressure and temperature.

Synchrotron X-ray diffraction shows that the new phase is cubic with a remarkably high bulk modulus of 372±5 GPa.

No thin film fabrication reported yet!

More noble metal nitrides synthesized

Experiments

- **PtN_2, (J. C. Crowhurst *et al*., Science 311, 1275 (2006).)**
- **IrN_2, OsN_2 (A. F. Young *et al*., Phys. Rev. Lett. 96, 155501 (2006).)**

Computations

- **IrN_2, OsN_2 (A. F. Young *et al*., Phys. Rev. Lett. 96, 155501 (2006).)**
- **PtN_2, (R. Yu *et al.,* Appl. Phys. Lett. 88, 51913 (2006).)**
- **PtN_2, (J. C. Crowhurst *et al*., Science 311, 1275 (2006).)**
- **PtN, (S. K. R. Patil *et al.,* Phys. Rev. B 73, 104118 (2006).)**

Results

- **Made in diamond anvil cells at 2000K and P = 50 GPa. Recovered at 300K and 0.1 MPa, ambient conditions.**
- **PtN_2 is now confirmed to be in pyrite phase.**
- **IrN_2, (hexagonal symmetry) and OsN_2 (orthorhombic symmetry) structures not fully confirmed.**
- **No thin film production method discovered!**

Fluorite(C1) Phase [MN_2]

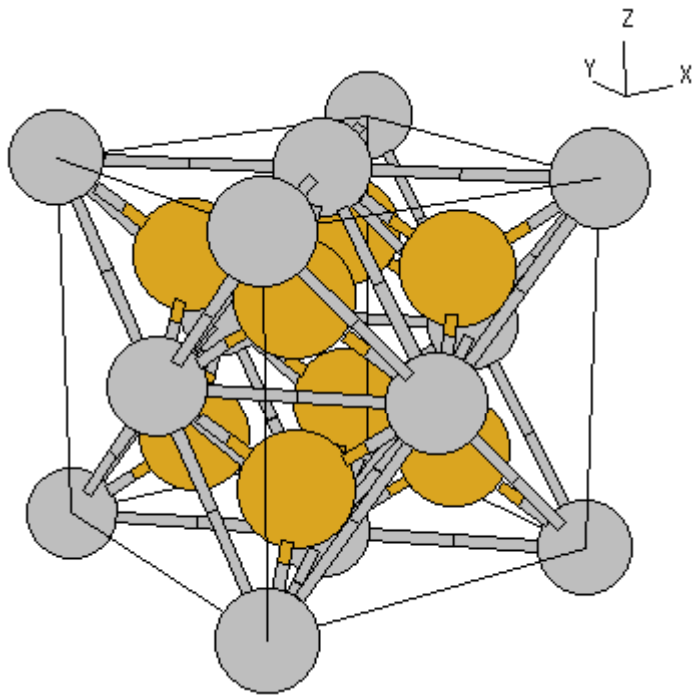

Lattice Vectors

$$\mathbf{A_1} = \tfrac{1}{2}\, a\, \mathbf{Y} + \tfrac{1}{2}\, a\, \mathbf{Z}$$

$$\mathbf{A_2} = \tfrac{1}{2}\, a\, \mathbf{X} + \tfrac{1}{2}\, a\, \mathbf{Z}$$

$$\mathbf{A_3} = \tfrac{1}{2}\, a\, \mathbf{X} + \tfrac{1}{2}\, a\, \mathbf{Y}$$

Basis Vectors

$$\mathbf{B_1} = 0$$

$$\mathbf{B_2} = +\tfrac{1}{4}\mathbf{A_1} + \tfrac{1}{4}\mathbf{A_2} + \tfrac{1}{4}\mathbf{A_3} = +\tfrac{1}{4}\, a\, \mathbf{X} + \tfrac{1}{4}\, a\, \mathbf{Y} + \tfrac{1}{4}\, a\, \mathbf{Z}$$

$$\mathbf{B_3} = -\tfrac{1}{4}\mathbf{A_1} - \tfrac{1}{4}\mathbf{A_2} - \tfrac{1}{4}\mathbf{A_3} = -\tfrac{1}{4}\, a\, \mathbf{X} - \tfrac{1}{4}\, a\, \mathbf{Y} - \tfrac{1}{4}\, a\, \mathbf{Z}$$

Metal

Nitrogen

Pyrite (C2) Phase [MN_2]

Lattice Vectors

$\mathbf{A}_1 = a\,\mathbf{X}$

$\mathbf{A}_2 = a\,\mathbf{Y}$

$\mathbf{A}_3 = a\,\mathbf{Z}$

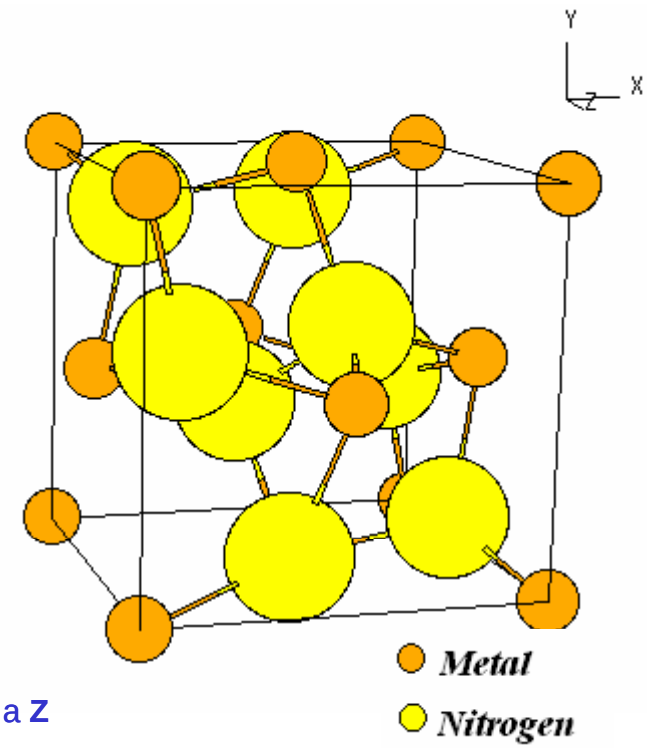

Basis Vectors

$\mathbf{B}_1 = 0$

$\mathbf{B}_2 = \frac{1}{2}\mathbf{A}_2 + \frac{1}{2}\mathbf{A}_3 = \frac{1}{2}a\,\mathbf{Y} + \frac{1}{2}a\,\mathbf{Z}$

$\mathbf{B}_3 = \frac{1}{2}\mathbf{A}_1 + \frac{1}{2}\mathbf{A}_3 = \frac{1}{2}a\,\mathbf{X} + \frac{1}{2}a\,\mathbf{Z}$

$\mathbf{B}_4 = \frac{1}{2}\mathbf{A}_1 + \frac{1}{2}\mathbf{A}_2 = \frac{1}{2}a\,\mathbf{X} + \frac{1}{2}a\,\mathbf{Y}$

$\mathbf{B}_5 = u\,\mathbf{A}_1 + u\,\mathbf{A}_2 + u\,\mathbf{A}_3 = u\,a\,\mathbf{X} + u\,a\,\mathbf{Y} + u\,a\,\mathbf{Z}$

$\mathbf{B}_6 = -u\,\mathbf{A}_1 - u\,\mathbf{A}_2 - u\,\mathbf{A}_3 = -u\,a\,\mathbf{X} - u\,a\,\mathbf{Y} - u\,a\,\mathbf{Z}$

$\mathbf{B}_7 = (\frac{1}{2} + u)\,\mathbf{A}_1 + (\frac{1}{2} - u)\,\mathbf{A}_2 - u\,\mathbf{A}_3 = (\frac{1}{2} + u)\,a\,\mathbf{X} + (\frac{1}{2} - u)\,a\,\mathbf{Y} - u\,a\,\mathbf{Z}$

$\mathbf{B}_8 = -(\frac{1}{2} + u)\,\mathbf{A}_1 - (\frac{1}{2} - u)\,\mathbf{A}_2 + u\,\mathbf{A}_3 = -(\frac{1}{2} + u)\,a\,\mathbf{X} - (\frac{1}{2} - u)\,a\,\mathbf{Y} + u\,a\,\mathbf{Z}$

$\mathbf{B}_9 = -u\,\mathbf{A}_1 + (\frac{1}{2} + u)\,\mathbf{A}_2 + (\frac{1}{2} - u)\,\mathbf{A}_3 = -u\,a\,\mathbf{X} + (\frac{1}{2} + u)\,a\,\mathbf{Y} + (\frac{1}{2} - u)\,a\,\mathbf{Z}$

$\mathbf{B}_{10} = u\,\mathbf{A}_1 - (\frac{1}{2} + u)\,\mathbf{A}_2 - (\frac{1}{2} - u)\,\mathbf{A}_3 = u\,a\,\mathbf{X} - (\frac{1}{2} + u)\,a\,\mathbf{Y} - (\frac{1}{2} - u)\,a\,\mathbf{Z}$

$\mathbf{B}_{11} = (\frac{1}{2} - u)\,\mathbf{A}_1 - u\,\mathbf{A}_2 + (\frac{1}{2} + u)\,\mathbf{A}_3 = (\frac{1}{2} - u)\,a\,\mathbf{X} - u\,a\,\mathbf{Z} + (\frac{1}{2} + u)\,a\,\mathbf{Z}$

$\mathbf{B}_{12} = -(\frac{1}{2} - u)\,\mathbf{A}_1 + u\,\mathbf{A}_2 - (\frac{1}{2} + u)\,\mathbf{A}_3 = -(\frac{1}{2} - u)\,a\,\mathbf{X} + u\,a\,\mathbf{Z} - (\frac{1}{2} + u)\,a\,\mathbf{Z}$

Pyrite Structure

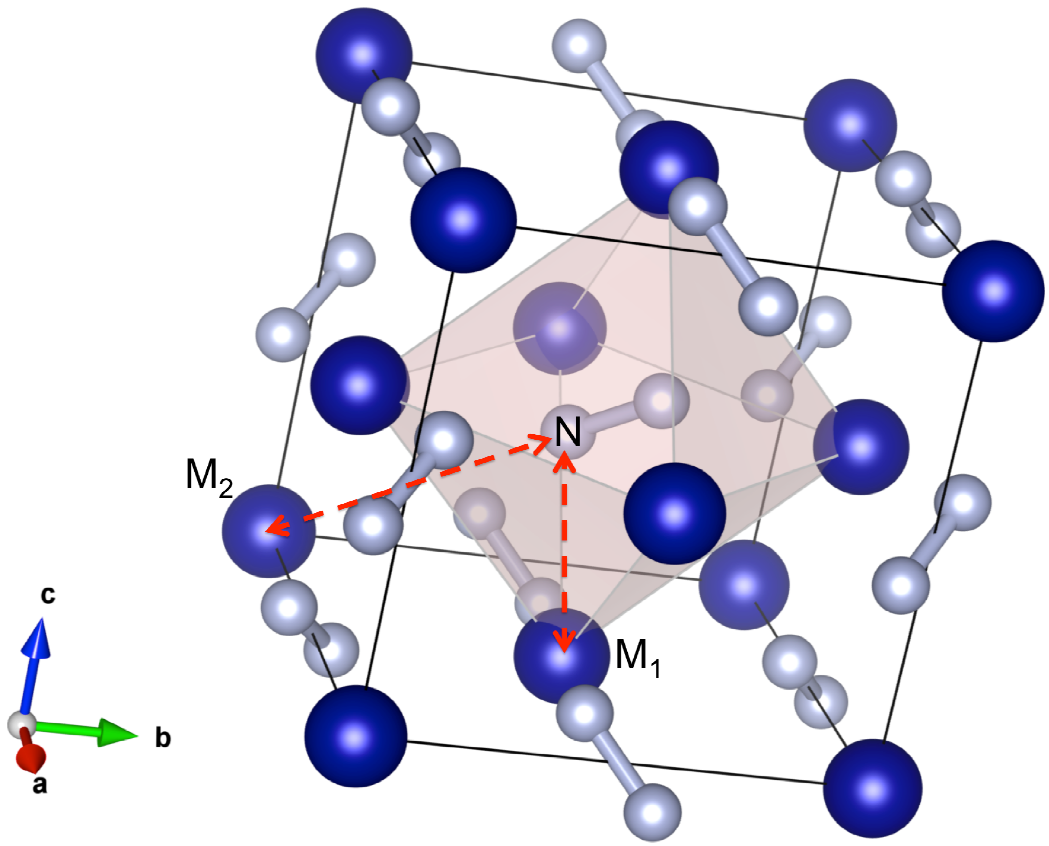

cubic $Pa\bar{3}$

PtN_2

a = 4.877 Å

Nitrogen atom at

(0.416, 0.416, 0.416)

Cohesive Energy of MN (M – metal)

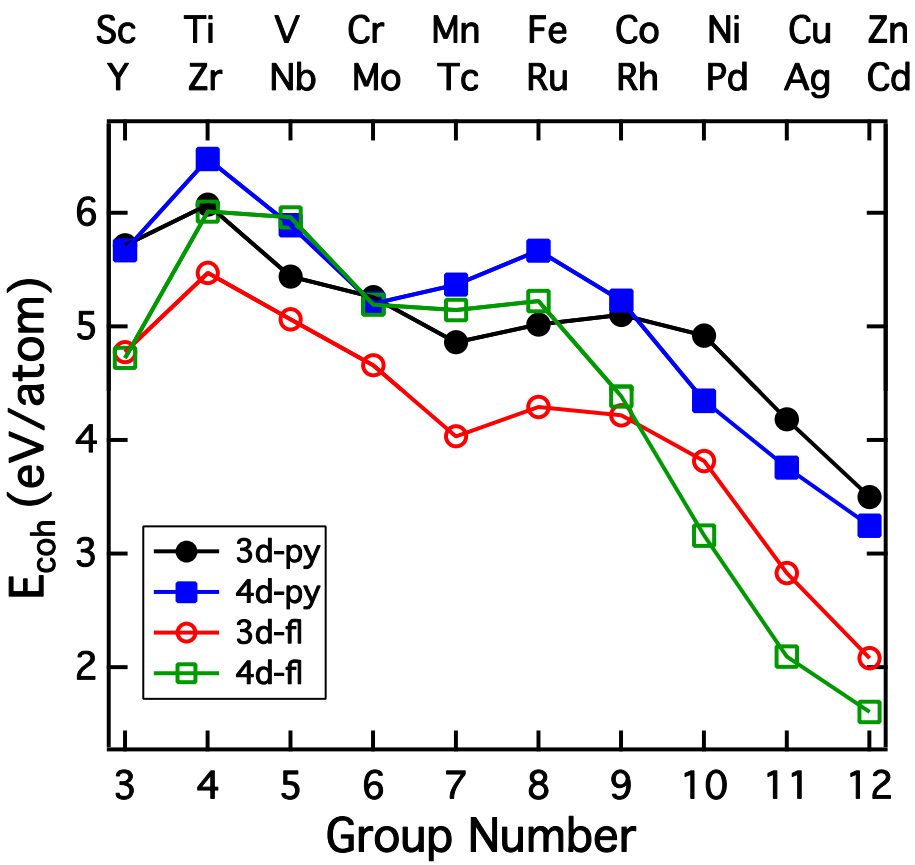

Cohesive energy E_{coh} of 3d, 4d transition metal nitrides in **pyrite** and **fluorite** structures

$E_{coh} = (E_M + E_N - E_{MN})/2$

The larger, the more stable thermodynamically

Fluorite phases are in general less stable than pyrite counterparts

Z. T. Y. Liu, D. Gall, and S. V. Khare, Phys. Rev. B **90**, 134102 (2014).

Elastic constants C_{11} - C_{12}, C_{44} and mechanical stability of the pyrite-type transition-metal pernitrides, MN_2. Mechanically stable phases are denoted as "S" and unstable ones as "U."

Group	M		C_{11} - C_{12} (GPa)		C_{44} (GPa)		Mechanical Stability	
3	Sc	Y	-32.7	-160.8	61.6	56.0	U	U
4	Ti	Zr	205.0	107.6	97.9	98.5	S	S
5	V	Nb	253.7	89.3	9.4	-38.4	S	U
6	Cr	Mo	287.7	241.3	61.4	-20.0	S	U
7	Mn	Tc	360.5	351.4	104.7	24.3	S	S
8	Fe	Ru	419.4	397.5	30.7	-52.7	S	U
9	Co	Rh	454.6	428.6	89.1	52.7	S	S
10	Ni	Pd	274.0	104.0	86.7	33.9	S	S
11	Cu	Ag	-24.5	5.0	29.2	12.0	U	S
12	Zn	Cd	112.4	85.9	57.7	14.2	S	S

Mechanically Stable pernitrides MN_2

Only 17 are stable

Transition metal elements

	1 H 1.00794																	2 He 4.002602
	3 Li 6.941	4 Be 9.012182											5 B 10.811	C 12.0107	7 N 14.00674	8 O 15.9994	9 F 18.9984032	10 Ne 20.1797
	11 Na 22.989770	12 Mg 24.3050											13 Al 26.581538	14 Si 28.0855	15 P 30.973761	16 S 32.066	17 Cl 35.4527	18 Ar 39.948
3d	19 K 39.0983	20 Ca 40.078	21 Sc 44.955910	22 Ti 47.867	23 V 50.9415	24 Cr 51.9961	25 Mn 54.938049	26 Fe 55.845	27 Co 58.933200	28 Ni 58.6534	29 Cu 63.545	30 Zn 65.39	31 Ga 69.723	32 Ge 72.61	33 As 74.92160	34 Se 78.96	35 Br 79.504	36 Kr 83.80
4d	37 Rb 85.4678	38 Sr 87.62	39 Y 88.90585	40 Zr 91.224	41 Nb 92.90638	42 Mo 95.94	43 Tc (98)	44 Ru 101.07	45 Rh 102.90550	46 Pd 106.42	47 Ag 196.56655	48 Cd 112.411	49 In 114.818	50 Sn 118.710	51 Sb 121.760	52 Te 127.60	53 I 126.90447	54 Xe 131.29
5d	55 Cs 132.90545	56 Ba 137.327	57 La 138.9055	72 Hf 178.49	73 Ta 180.94.79	74 W 183.84	75 Re 186.207	76 Os 190.23	77 Ir 192.217	78 Pt 195.078	79 Au 196.56655	80 Hg 200.59	81 Tl 204.3833	82 Pb 207.2	83 Bi 208.58038	84 Po (209)	85 At (210)	86 Rn (222)
	87 Fr (223)	88 Ra (226)	89 Ac (227)	104 Rf (261)	105 Db (262)	106 Sg (263)	107 Bh (262)	108 Hs (265)	109 Mt (266)	110 (269)	111 (272)	112 (277)		114 (289) (287)		116 (289)		118 (293)

58 Ce 140.116	59 Pr 140.50765	60 Nd 144.24	61 Pm (145)	62 Sm 150.36	63 Eu 151.964	64 Gd 157.25	65 Tb 158.92534	66 Dy 162.50	67 Ho 164.93032	68 Er 167.26	69 Tm 168.93421	70 Yb 173.04	71 Lu 174.967
90 Th 232.0381	91 Pa 231.035888	92 U 238.0289	93 Np (237)	94 Pu (244)	95 Am (243)	96 Cm (247)	97 Bk (247)	98 Cf (251)	99 Es (252)	100 Fm (257)	101 Md (258)	102 No (259)	103 Lr (262)

Z. T. Y. Liu, D. Gall, and S. V. Khare, Phys. Rev. B **90**, 134102 (2014).

Density of states (DOS) at E_F and elastic constant C_{44} of pyrite-type 3d, 4d transition metal pernitrides MN_2

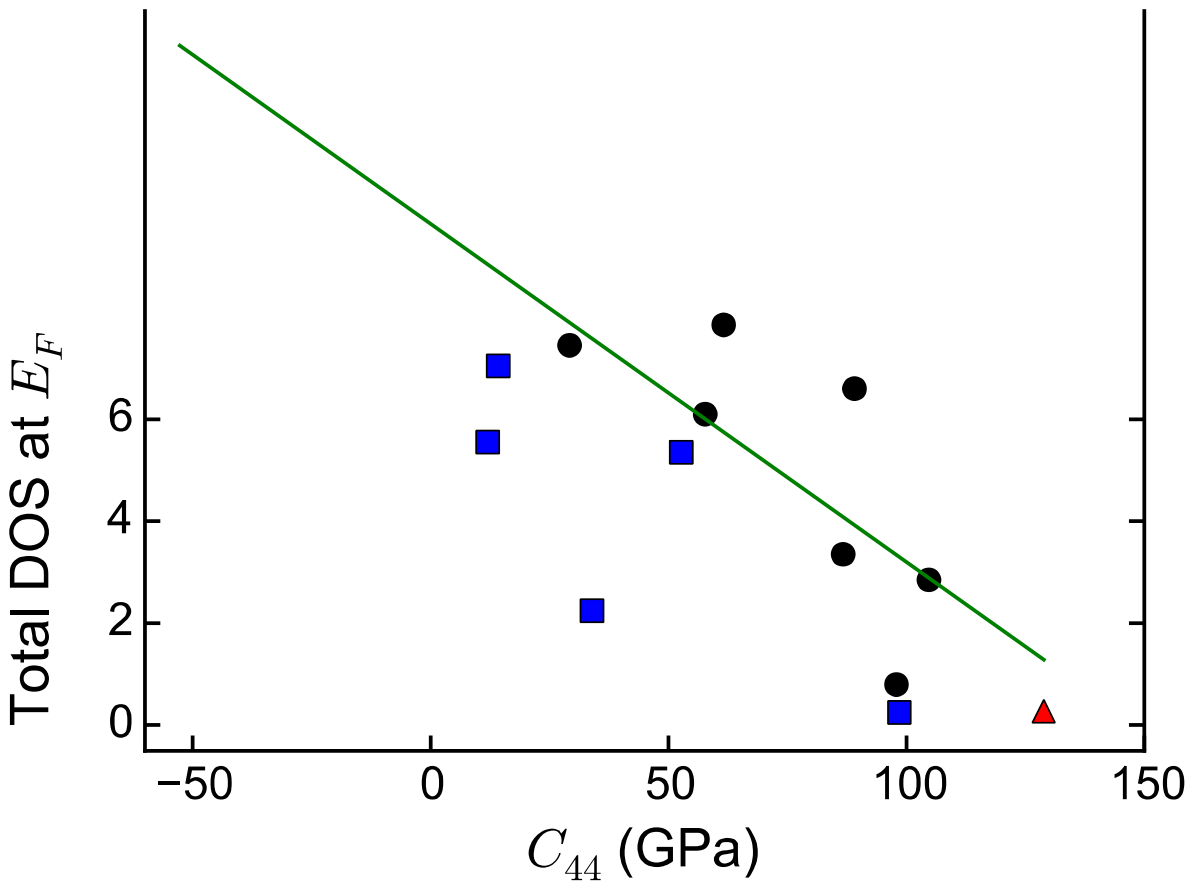

Z. T. Y. Liu, D. Gall, and S. V. Khare, Phys. Rev. B **90**, 134102 (2014).

Density of States (DOS) and Elastic Constant C_{44}

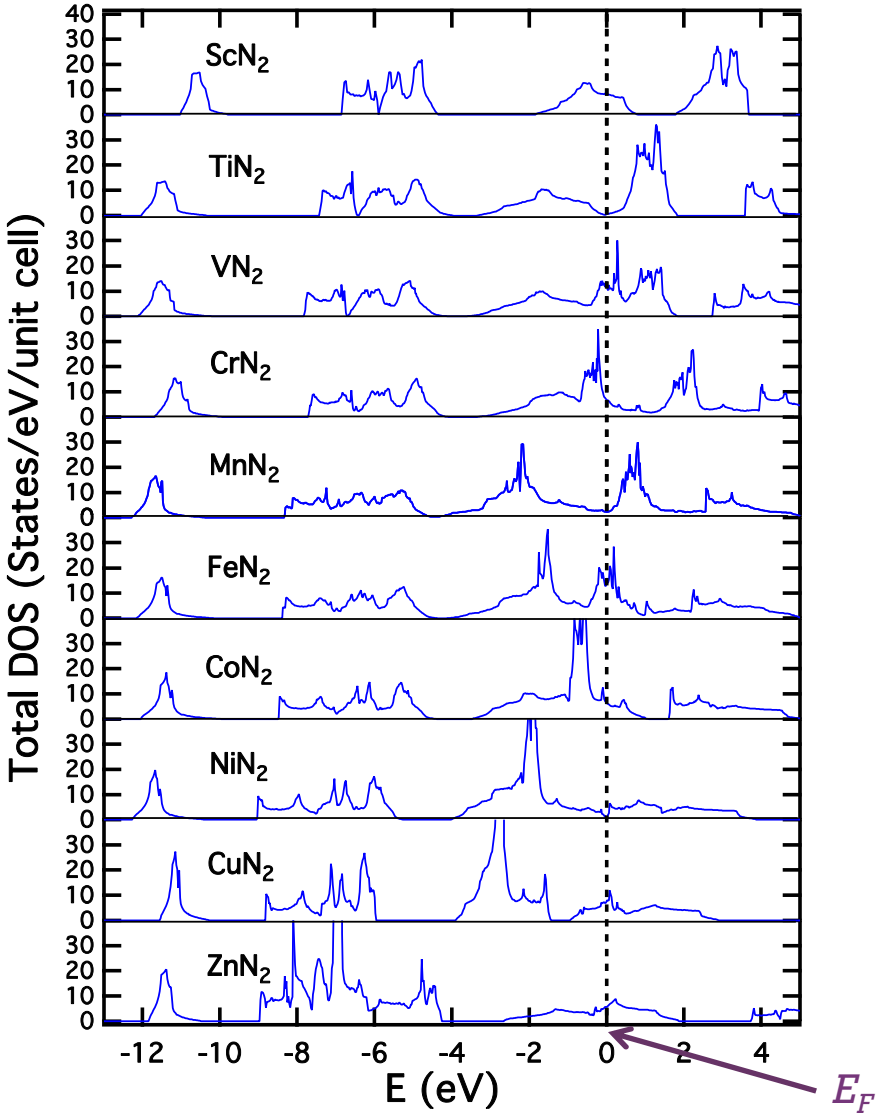

Total DOS of **pyrite**-type 3d transition metal pernitrides MN_2.

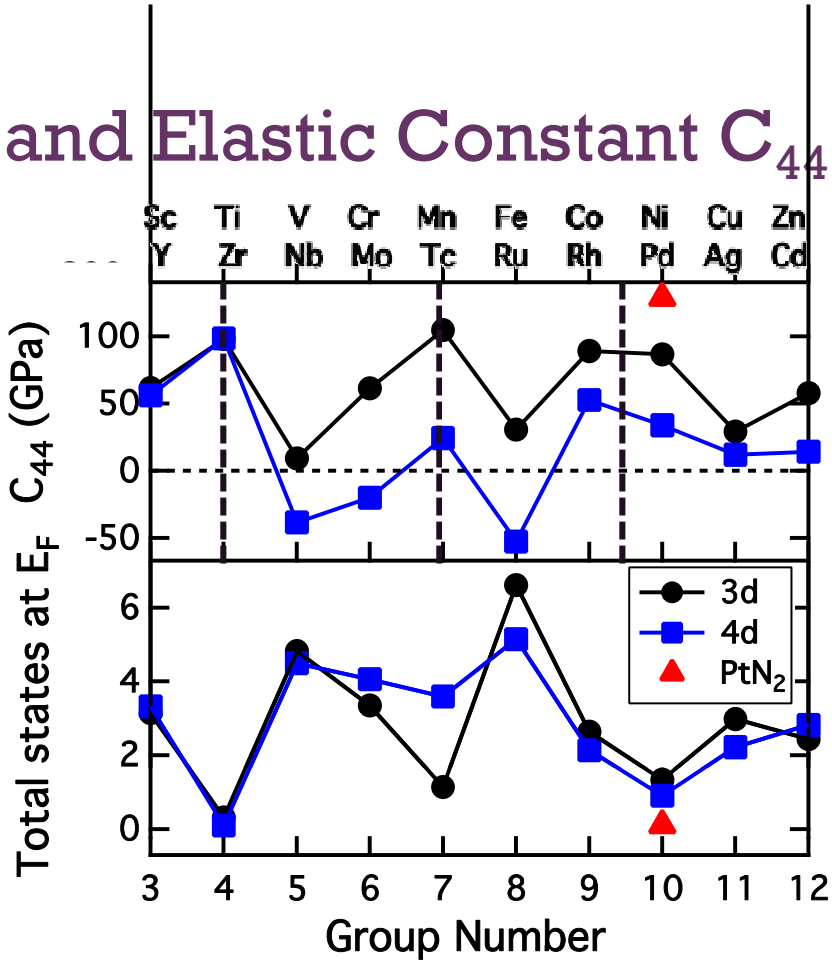

Elastic constant C_{44} and Total DOS at E_F of **pyrite**-type 3d, 4d transition metal pernitrides MN_2.

- Left shift and narrowing to accommodate more electrons.
- E_F (Fermi energy) can land on peaks, valleys or plateaus.

- Total DOS at E_F indicates metallicity.
- C_{44} indicates stability and positively correlates with H_V.

Density of States (DOS) and Elastic Constant C_{44}

5d period progression

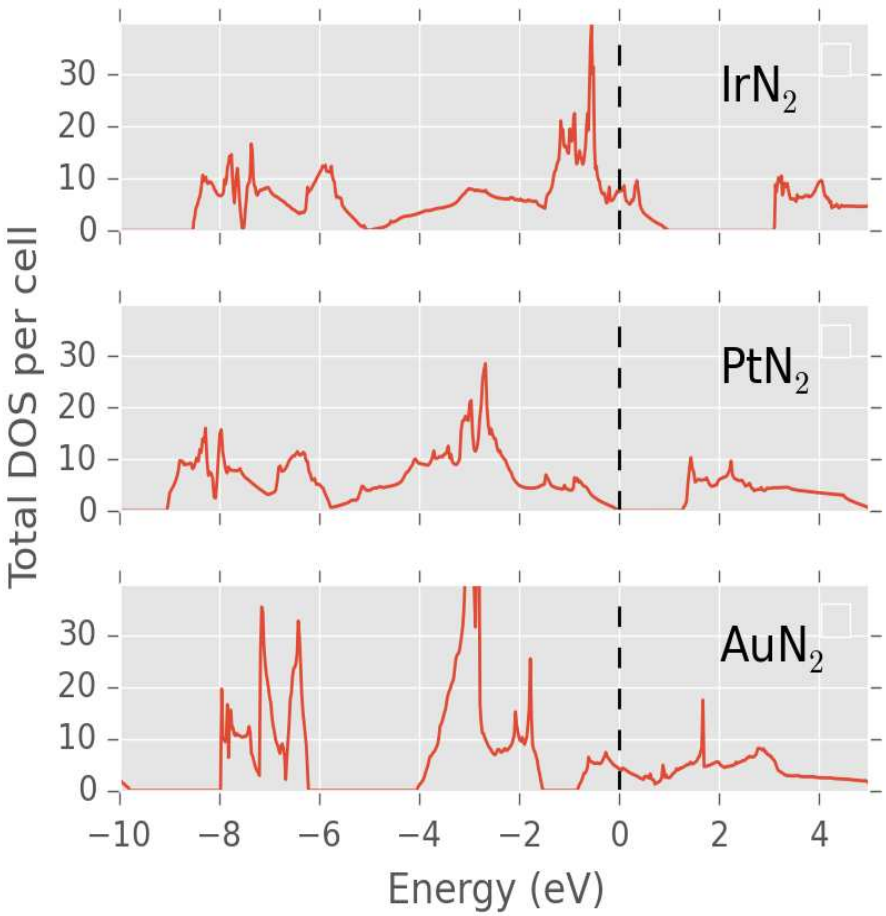

IrN_2 and PtN_2 are mechanically stable, but AuN_2 is not.

Judging by the DOS at E_F, PtN_2 is a semiconductor but neither IrN_2 nor AuN_2.

It is the left shift and width-narrowing behavior of DOS, placing a gap of states at the E_F of PtN_2.

Density of States (DOS) and Elastic Constant C_{44}

Group 10 progression

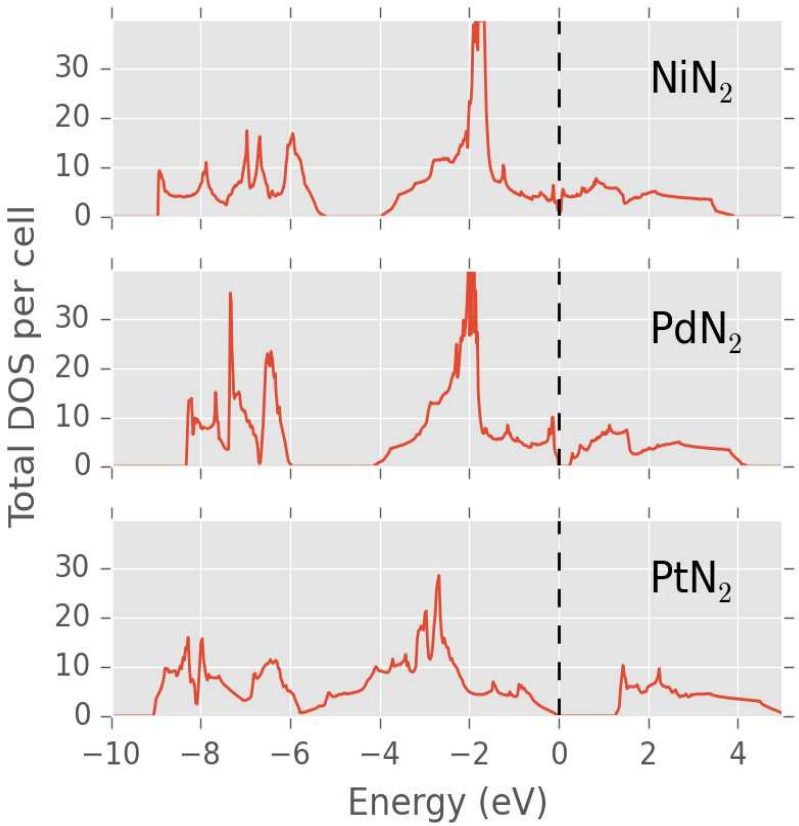

Group 4 progression

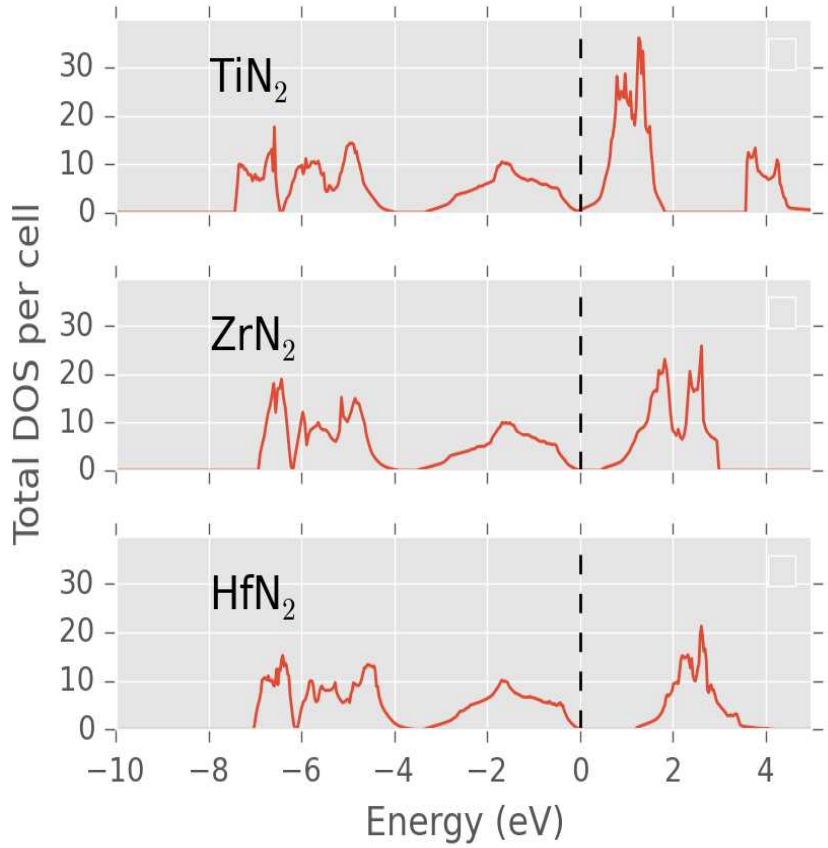

NiN_2: small notch between the two peaks at E_F

PdN_2 or PtN_2 : semiconductors with band gaps

TiN_2: small notch between the two peaks at E_F

ZrN_2 or HfN_2 : semiconductors with band gaps

Density of States (DOS) and Elastic Constant C_{44}

Conclusion:

As the transition metal choice moves in the periodic table, the pernitride demonstrates metallic or non-metallic behavior, depending on the relative position of E_F in DOS.

The mechanical stability and shear related mechanical properties (like hardness) can be anti-correlated with DOS at E_F, an indicator of metallicity.

Z. T. Y. Liu, D. Gall, and S. V. Khare, Phys. Rev. B **90**, 134102 (2014).

Projected COHP

Plane Wave DFT codes express information in the reciprocal space.

Crystal orbital Hamilton population (COHP) analysis is a DFT successor of the familiar crystal orbital overlap population (COOP) concept, based on extended Hückel theory.

COHP is a partitioning of the band-structure energy in terms of orbital-pair contributions

It is therefore based on a local bases.

Projecting plane waves onto local bases gives projected COHP.

V. L. Deringer, A. L. Tchougreeff and R. Dronskowski, J. Phys. Chem. A **115**, 5461 (2011).

pCOHP In Pyrite-Type PtN_2

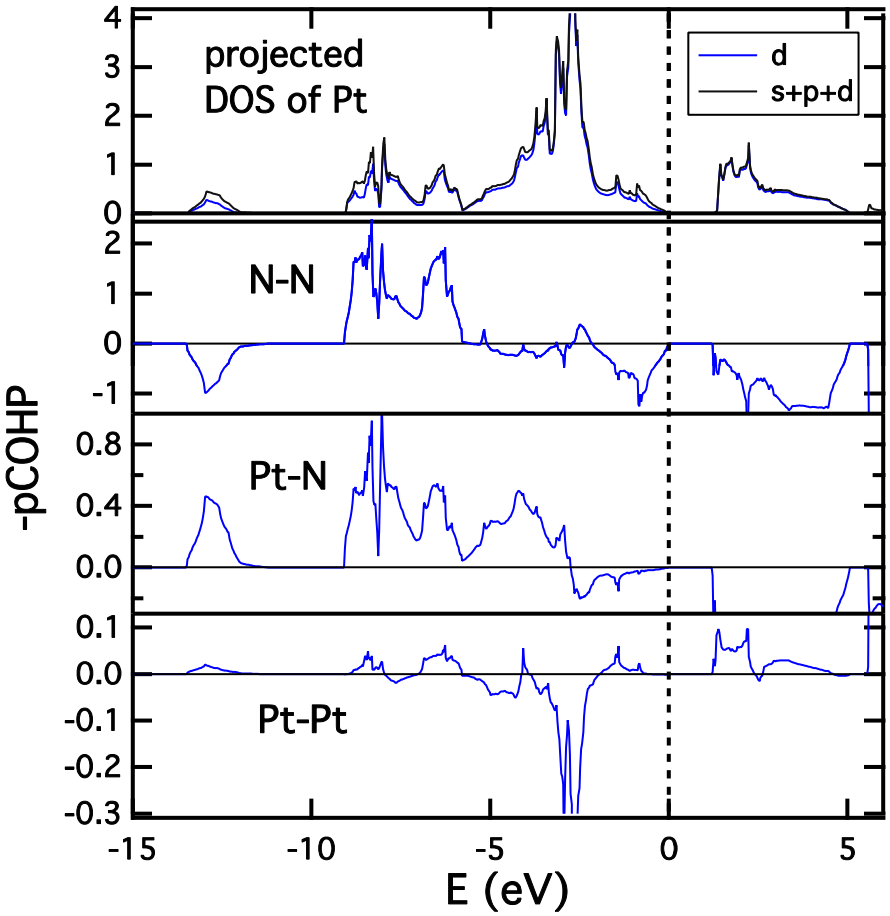

Mostly d states compared with s + p

N-N and Pt-N bonds lower the energy

Anti-bonding region of N-N

Pt-Pt anti-bonding

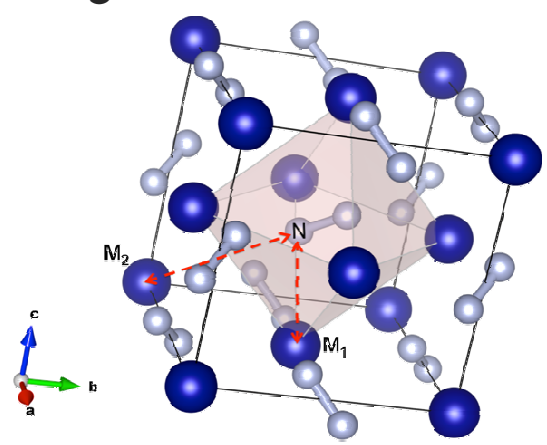

Z. T. Y. Liu, D. Gall, and S. V. Khare, Phys. Rev. B **90**, 134102 (2014).

Equation For Calculating Vickers Hardness (H_V)

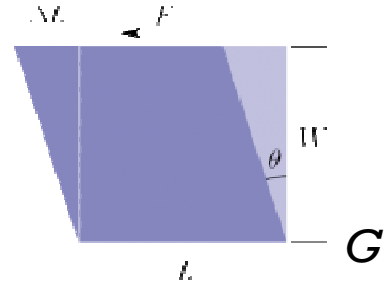

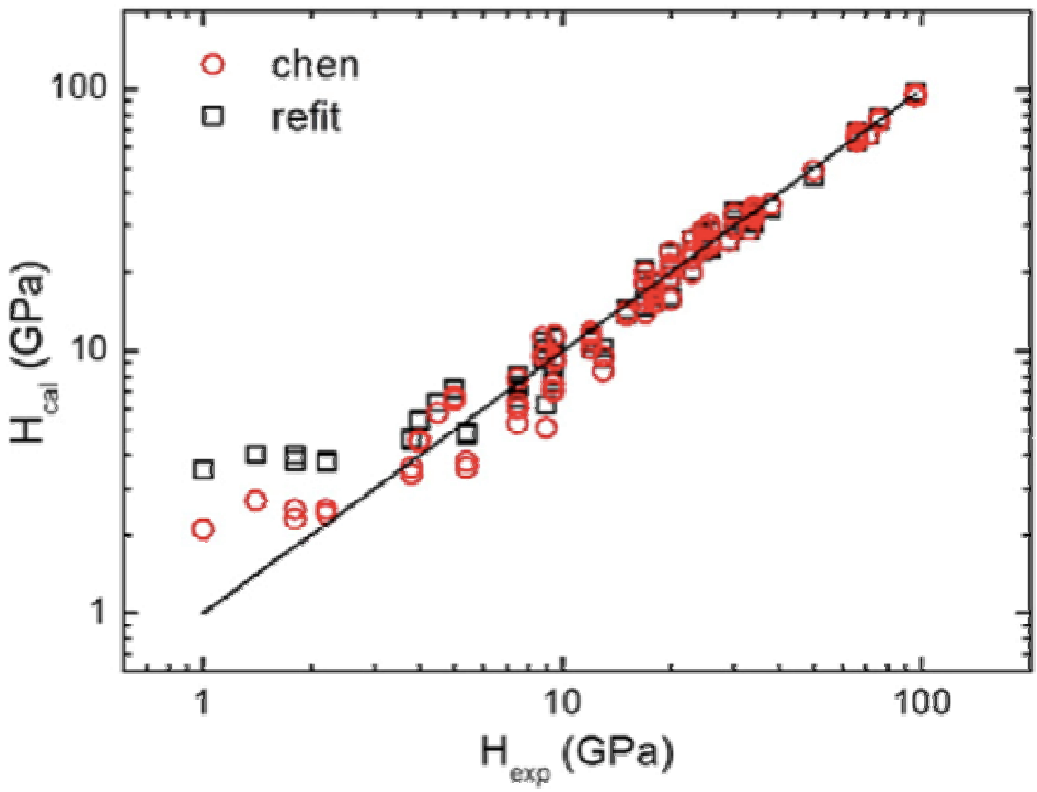

$$H_V = 0.92k^{1.137}G^{0.708}$$

$k = G/B$

k - Pugh's ratio
G - shear modulus

Data points (40+ compounds):

Covalent: C, Si, BN…
Ionic: NaCl, KBr…
Metallic glasses

Figure adapted from Tian *et al.*
Y. Tian, B. Xu, and Z. Zhao, Int. J. Refract. Met. Hard Mater. **33**, 93 (2012).
X. Q. Chen, H. Y. Niu, D. Z. Li and Y. Y. Li, Intermetallics **19**, 1275 (2011).

Change of Metal Bond Strength Under Shear Stress

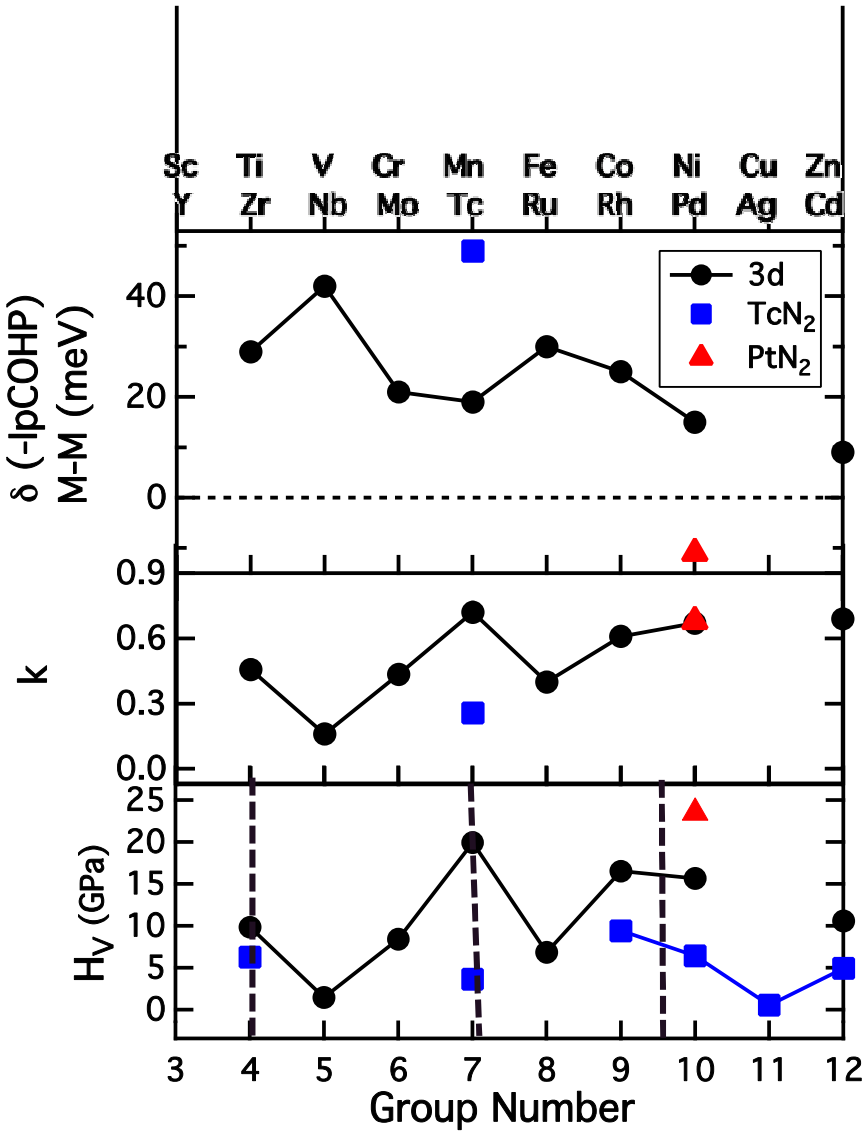

3d, 4d **pyrite**-type transition metal pernitrides.
PtN_2 being super-hard is shown distinctly.

- ***k* = *G/B*** - Pugh's ratio
- H_V - Vickers hardness

- **M-M** metal to metal bond.
- **pCOHP** – projected Crystal Orbital Hamilton Population.
- **IpCOHP** – Integrated pCOHP.
- **-IpCOHP** - a measurement of **bond strength.**
- **δ(-IpCOHP)** – the change of **bond strength** with a C_{44} shearing strain, [110]-oriented.

Anti-correlation between δ(-IpCOHP) of M-M and *k*, H_V.

If M-M bond increases strength with shear, then the material is easier to shear, more ductile, and less hard.

Z. T. Y. Liu, D. Gall, and S. V. Khare, Phys. Rev. B **90**, 134102 (2014).

Charge Density Plot

Charge transfer (ionicity) does not indicate hardness

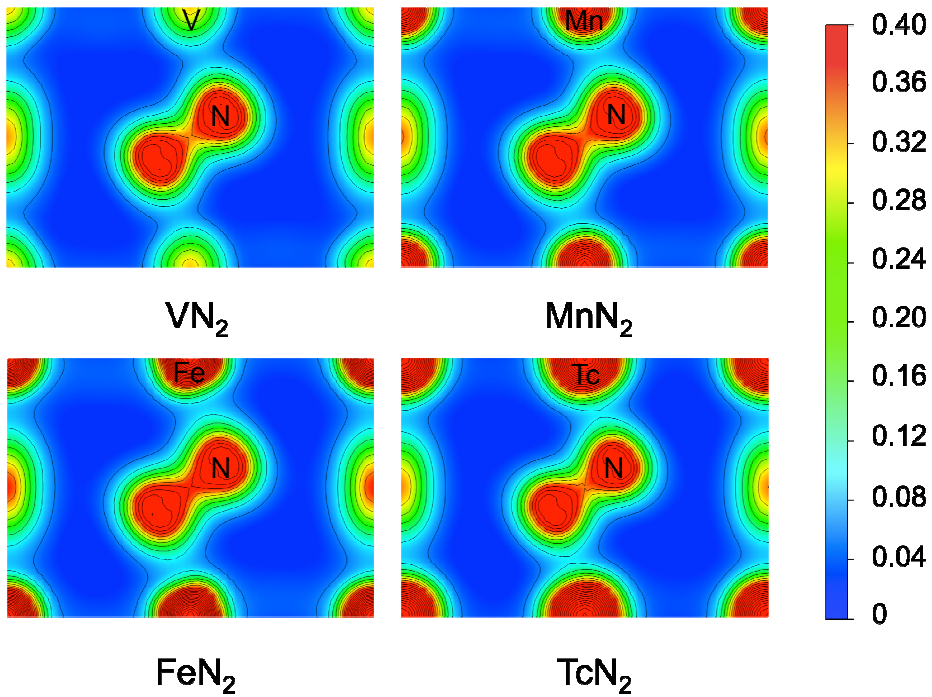

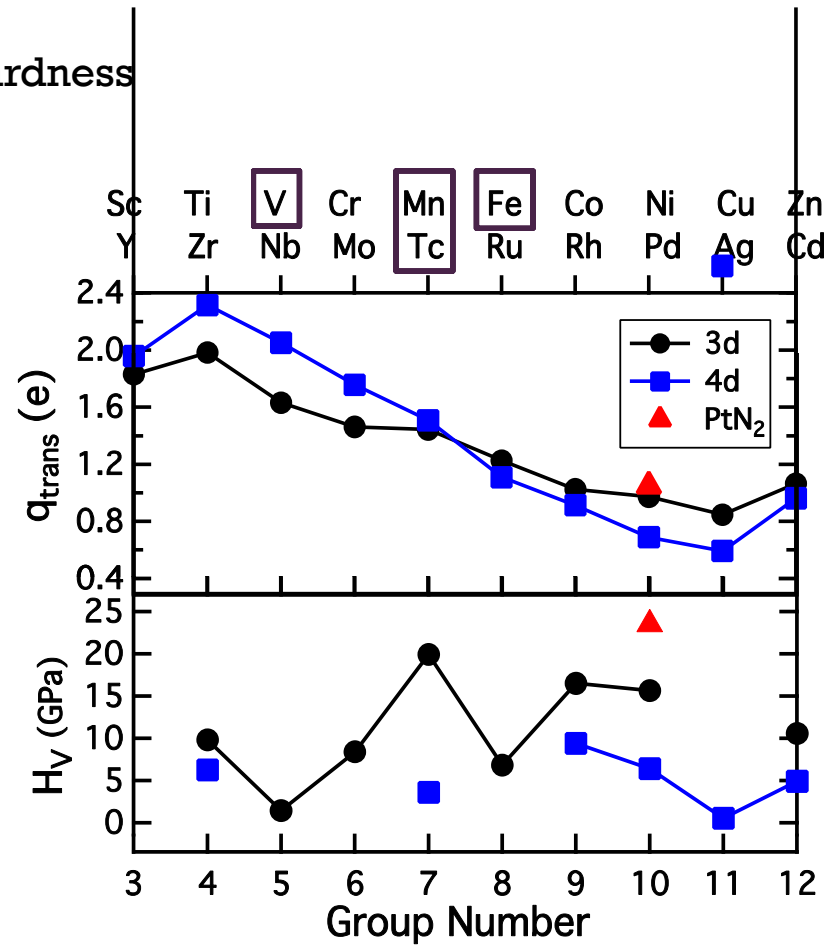

- More charge transfer, longer the bond, and less the density in between (suggesting strength).
- No correlation with shear related mechanical properties.

Charge Transfer

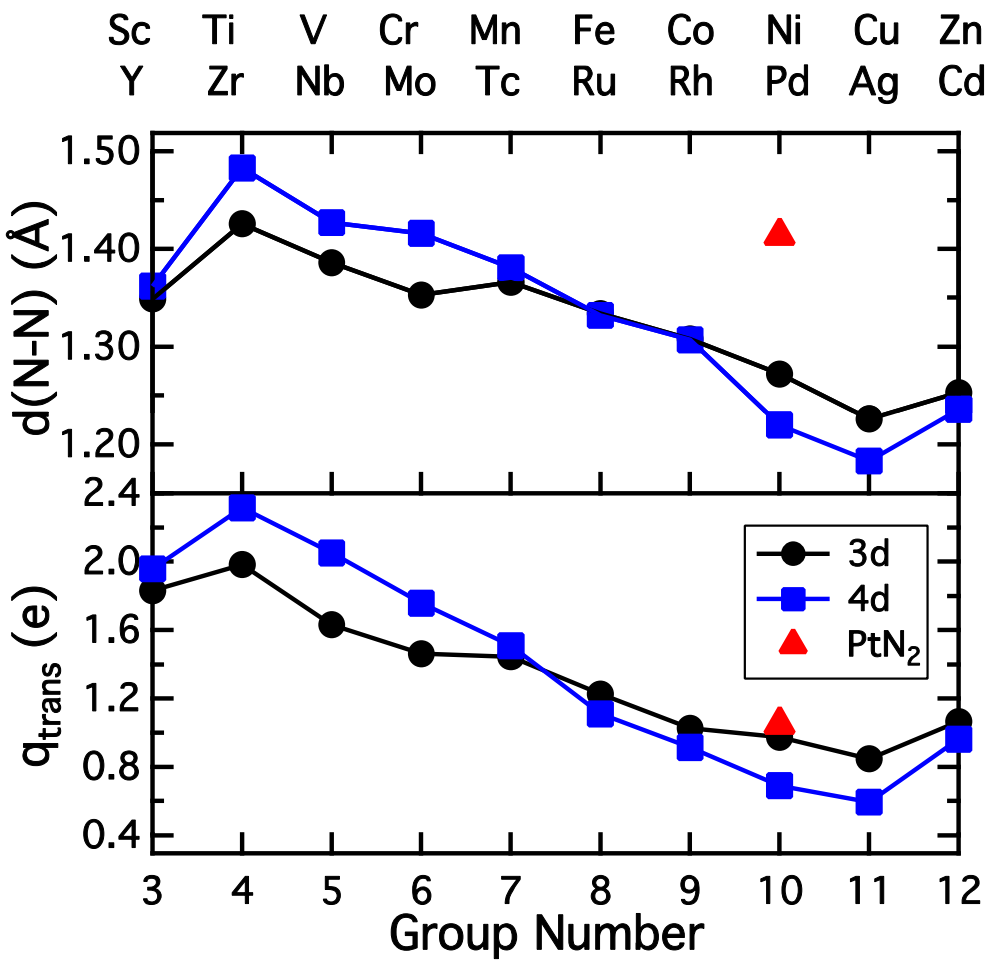

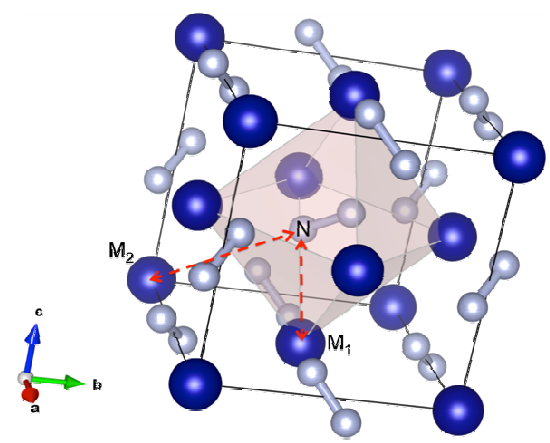

Correlation between d(N-N) and q_{trans} (Bader charge transfer)

Coulomb repulsion induced elongation

Z. T. Y. Liu, D. Gall, and S. V. Khare, Phys. Rev. B **90**, 134102 (2014).

Bond Length and Charge States

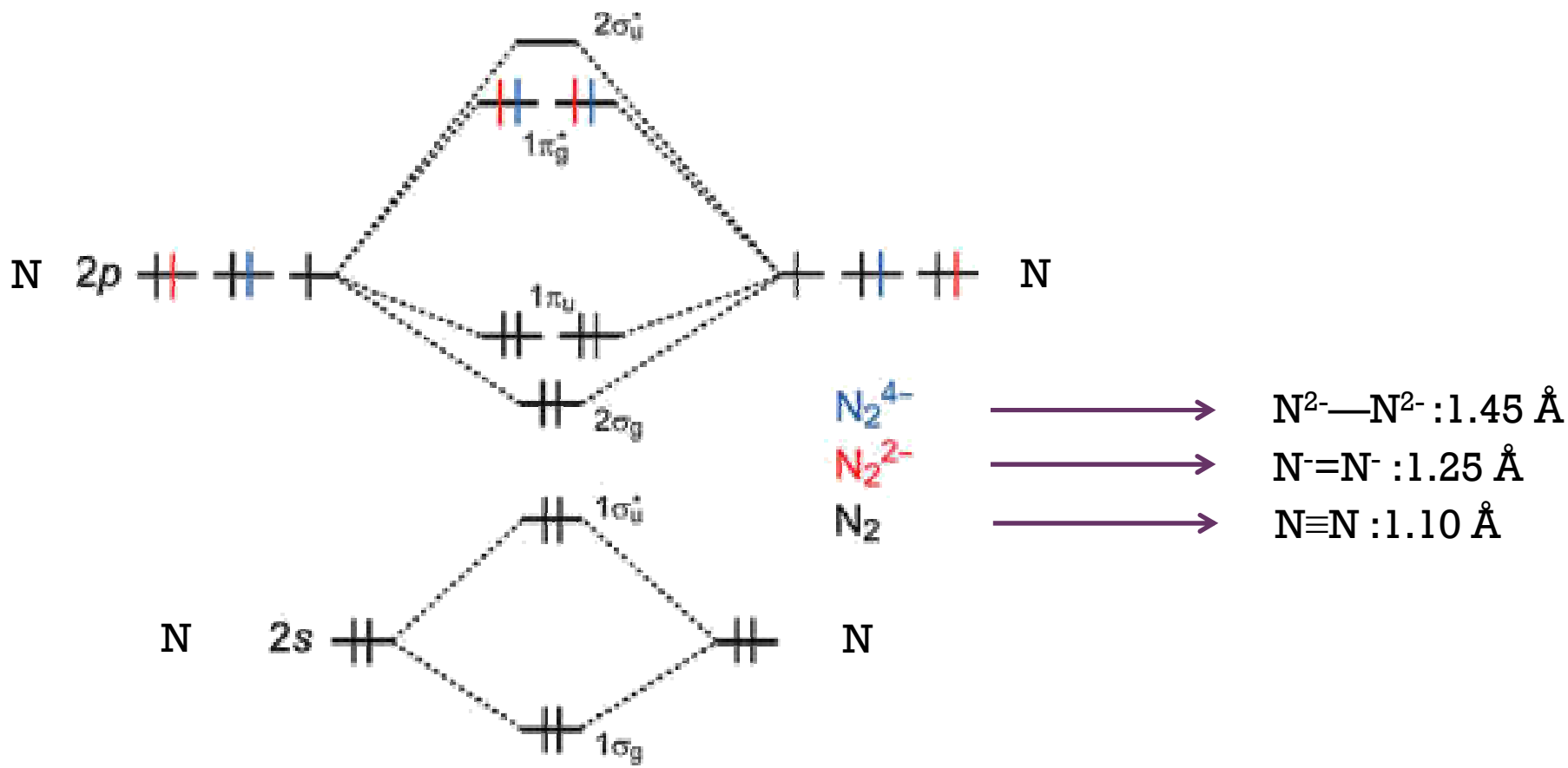

M. Wessel and R. Dronskowski, JACS **132**, 2421 (2010).

Summary I

1. Often cited optimum valence electron concentration (VEC) for shear-related mechanical properties like H_V found in rocksalt-type early transition metal nitrides (8.5 e/formula unit) differs with structures.

2. Shear related properties can be correlated with total density of states (DOS) at E_F, an indicator of metallicity.

Z. T. Y. Liu, D. Gall, and S. V. Khare, Phys. Rev. B **90**, 134102 (2014).

Summary II

3. The change in M-M bond strength under a shearing strain indicated by crystal orbital Hamilton population (COHP) is predictive of hardness. This is a direct connection between a specific bond and shear related mechanical properties.

4. Charge transfer from M to N controls the length of the N-N bond, dominantly by providing Coulomb repulsion between the pairing N atoms. PtN_2 has additional anti-bonding contribution.

Z. T. Y. Liu, D. Gall, and S. V. Khare, Phys. Rev. B **90**, 134102 (2014).

Community-Based Ceramics Database

http://astro1.panet.utoledo.edu/ceramicsdb

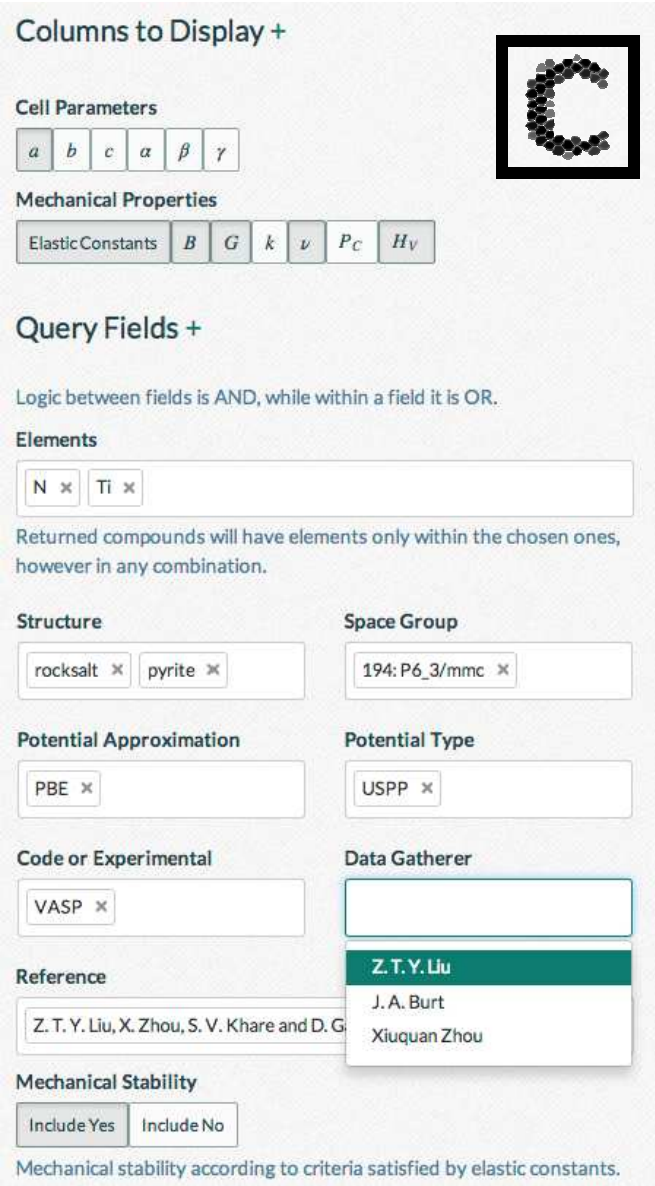

Name	University	Entries Contributed
Z. T. Y. Liu	University of Toledo	202
J. A. Burt	Minnesota State University, Mankato	157
Xiuquan Zhou	University of Maryland College Park	29

Centralized platform for crystal data related to **structure**, **composition**, **elastic**, and **mechanical** (more in future) properties for **ceramic** materials

Compiled from the **literature**, past, present and future

Community-based: participation and contribution expected to populate the database

User-friendly and versatile **searching** capability

User-specified **tabular** display capability for search results

Graphical display of trends search results

Provides direct links to the original papers and correspondence information of authors

Graphical Display of Search Results

Draw Figure

Display

First select rows (by checkbox in the table)

Selected rows (by ID)

1, 2, 3, 4, 5, 6, 7, 8, 9, 10, 11, 12, 13, 14, 15, 16, 17, 18, 19, 20

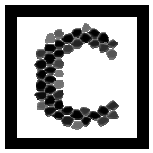

Now select a column

a | B | G | ν | H_V

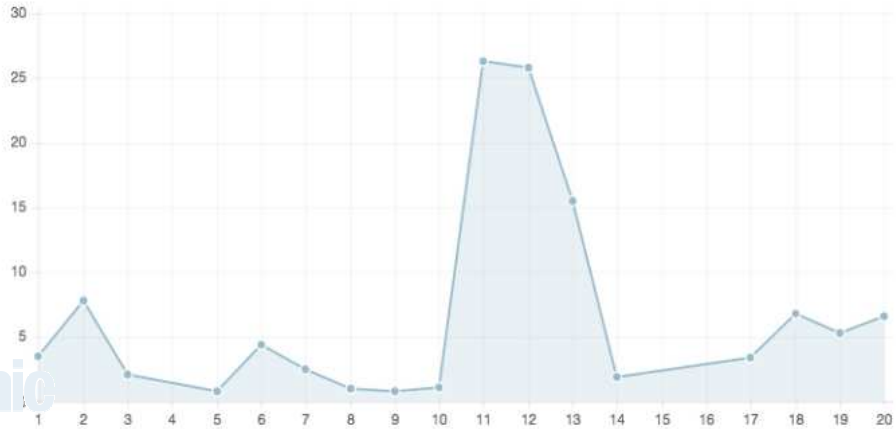

bilbao crystallographic server

www.cryst.ehu.es

ID	Structure	Space Group	Formula	a (Å)	Elastic Constants (GPa)	B (GPa)	G (GPa)	ν	H_V (GPa)	Potential Approx.	Potential Type	Code Package	Reference
1	zinc blende	216: *F-43m* Cubic	ScN	4.84	C11 = 186.9, C12 = 140.9, C44 = 73.8	156.2	46.3	0.37	3.5	LDA	USPP	VASP	Z. T. Y. Liu, X. Zhou, S. V. Khare and D. Gall, *Journal of P*
2	zinc blende	216: *F-43m* Cubic	TiN	4.529	C11 = 322.2, C12 = 176.4, C44 = 103.1	225.0	89.7	0.32	7.8	LDA	USPP	VASP	Z. T. Y. Liu, X. Zhou, S. V. Khare and D. Gall, *Journal of P*
3	zinc blende	216: *F-43m* Cubic	VN	4.368	C11 = 346.8, C12 = 229.4, C44 = 43.2	268.5	48.9	0.41	2.1	LDA	USPP	VASP	Z. T. Y. Liu, X. Zhou, S. V. Khare and D. Gall, *Journal of P*
4	zinc blende	216: *F-43m* Cubic	CrN	4.262	C11 = 361.7, C12 = 258.7, C44 = -77.9	–	–	–	–	LDA	USPP	VASP	Z. T. Y. Liu, X. Zhou, S. V. Khare and D. Gall, *Journal of P*
5	zinc blende	216: *F-43m* Cubic	MnN	4.188	C11 = 372.7, C12 = 279.7, C44 = 24.0	310.7	31.4	0.45	0.8	LDA	USPP	VASP	Z. T. Y. Liu, X. Zhou, S. V. Khare and D. Gall, *Journal of P*
6	zinc blende	216: *F-43m* Cubic	FeN	4.16	C11 = 379.2, C12 = 282.8, C44 = 114.2	314.9	80.8	0.38	4.4	LDA	USPP	VASP	Z. T. Y. Liu, X. Zhou, S. V. Khare and D. Gall, *Journal of P*
7	zinc blende	216: *F-43m* Cubic	CoN	4.177	C11 = 347.4, C12 = 266.0, C44 = 71.2	293.1	56.9	0.41	2.5	LDA	USPP	VASP	Z. T. Y. Liu, X. Zhou, S. V. Khare and D. Gall, *Journal of P*
8	zinc blende	216: *F-43m* Cubic	NiN	4.241	C11 = 278.1, C12 = 246.2, C44 = 49.9	256.8	31.6	0.44	1.0	LDA	USPP	VASP	Z. T. Y. Liu, X. Zhou, S. V. Khare and D. Gall, *Journal of P*
9	zinc blende	216: *F-43m* Cubic	CuN	4.344	C11 = 222.4, C12 = 199.9, C44 = 41.1	207.4	24.5	0.44	0.8	LDA	USPP	VASP	Z. T. Y. Liu, X. Zhou, S. V. Khare and D. Gall, *Journal of P*
10	zinc blende	216: *F-43m* Cubic	ZnN	4.472	C11 = 178.0, C12 = 159.4, C44 = 47.4	165.6	25.1	0.43	1.1	LDA	USPP	VASP	Z. T. Y. Liu, X. Zhou, S. V. Khare and D. Gall, *Journal of P*
11	rocksalt	225: *Fm-3m* Cubic	ScN	4.463	C11 = 470.1, C12 = 99.4, C44 = 164.3	223.0	172.4	0.19	26.3	LDA	USPP	VASP	Z. T. Y. Liu, X. Zhou, S. V. Khare and D. Gall, *Journal of P*
12	rocksalt	225: *Fm-3m* Cubic	TiN	4.184	C11 = 712.3, C12 = 123.2, C44 = 171.1	319.6	213.0	0.23	25.8	LDA	USPP	VASP	Z. T. Y. Liu, X. Zhou, S. V. Khare and D. Gall, *Journal of P*
13	rocksalt	225: *Fm-3m* Cubic	VN	4.057	C11 = 751.1, C12 = 178.9, C44 = 126.6	369.6	176.7	0.29	15.5	LDA	USPP	VASP	Z. T. Y. Liu, X. Zhou, S. V. Khare and D. Gall, *Journal of P*
14	rocksalt	225: *Fm-3m* Cubic	CrN	3.987	C11 = 702.8, C12 = 227.1, C44 = 9.3	385.7	57.9	0.43	1.9	LDA	USPP	VASP	Z. T. Y. Liu, X. Zhou, S. V. Khare and D. Gall, *Journal of P*
15	rocksalt	225: *Fm-3m* Cubic	MnN	3.945	C11 = 682.1, C12 = 241.6, C44 = -13.3	–	–	–	–	LDA	USPP	VASP	Z. T. Y. Liu, X. Zhou, S. V. Khare and D. Ga *Journal of P*

dx.doi.org/10.1088/0953-8984/26/2/025404

Thank you!

VASP input parameters

Density functional theory (DFT) calculation

Ultrasoft Vanderbilt pseudo-potentials (US-PP)

Generalized gradient approximation: GGA (PW91)

450 eV kinetic energy cutoff

12 x 12 x 12 k-point Monkhorst-Pack mesh

Electronic loop: energetic convergence 10^{-4} eV

Ionic loop: force convergence 0.01 eV/Å

Difference in B and G

$B = (C_{11} + 2C_{12})/3$

$G_v = [(C_{11} - C_{12}) + 3C_{44}]/5$

$G_R = [5(C_{11} - C_{12})C_{44}]/[4C_{44} + 3(C_{11} - C_{12})]$

$G = G_{VRH} = (G_v + G_R)/2$

$k = G/B$

Difference in *B* and *G*

Bulk modulus (*B*) only measures the resistance to isotropic hydrostatic pressure, while shear modulus (*G*) measures the resistance to anisotropic shear strain.

TiN (*G*: 187.2 GPa, *B*: 318.3 GPa, H_V: 23 GPa)

β-SiC (*G*: 191.4 GPa, *B*: 224.7 GPa, H_V: 34 GPa)

Gao FM, He JL, Wu ED, Lu SM, Yu LD, Li DC, et al. Phys Rev Lett 2003;91: 015502.
Gou HY, Hou L, Zhang JW, Gao FM. Appl Phys Lett 2008;92:241901.

Formulation for H_V (Vickers Hardness)

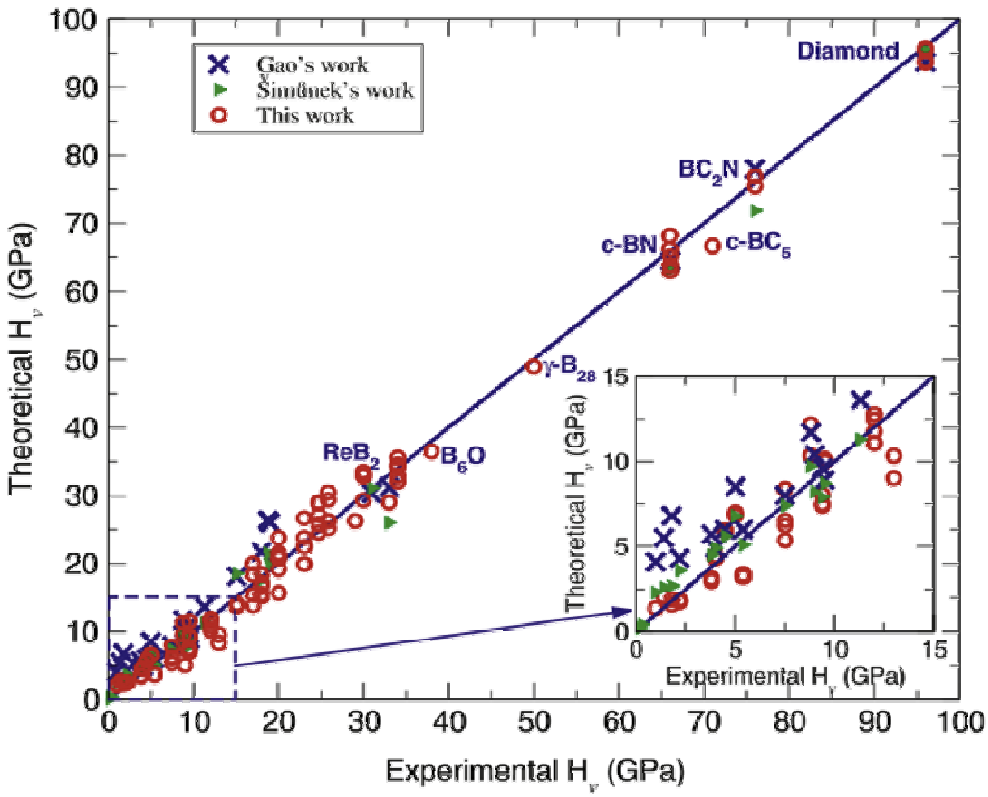

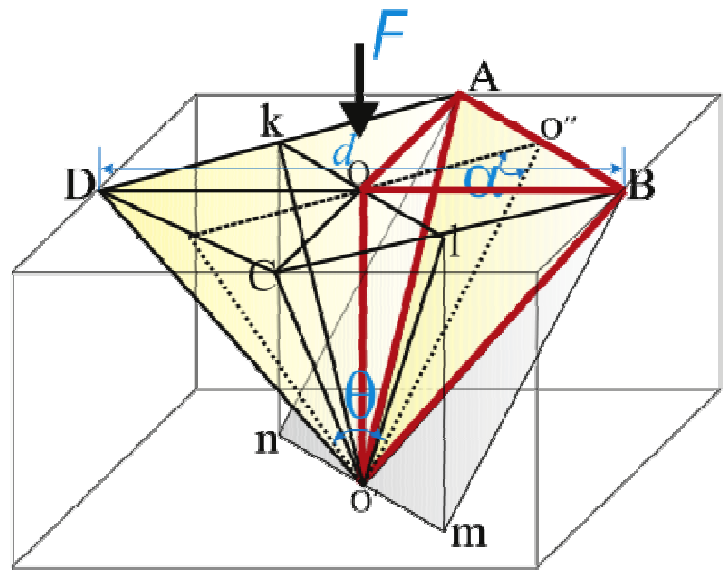

$$H_V = 2\left(k^2 G\right)^{0.585} - 3$$

X. Q. Chen *et al.*, Intermetallics **19**, 1275 (2011)

Crystal	H_{Exp} (GPa)	H_{Tian} (GPa)	$H_{Simunek}$ (GPa)	H_{Xue} (GPa)	H_{Chen} (GPa)
C	96[a]	93.6	95.4[b]	90[e]	94.6[f]
Si	12[a]	13.6	11.3[b]	14[e]	11.2[f]
Ge	8.8[b]	11.7	9.7[b]	11.4[e]	10.4[f]
SiC	31[b]	30.3	31.1[b]	27.8[e]	33.8[f]
BN	63[a]	64.5	63.2[b]	47.7[e]	65.3[f]
BP	33[a]	31.2	26[b]	24.9[e]	29.3[f]
BAs	19[b]	26	19.9[b]	21.1[e]	–
AlN	18[a]	21.7	17.6[b]	14.5[e]	16.8[f]
AlP	9.4[a]	9.6	7.9[b]	7.4[e]	7.2[f]
AlAs	5.0[a]	8.5	6.8[b]	6.3[e]	6.6[f]
AlSb	4.0[a]	4	4.9[b]	4.9[e]	4.4[f]
GaN	15.1[a]	18.1	18.5[b]	13.5[e]	13.9[f]
GaP	9.5[a]	8.9	8.7[b]	8[e]	9.9[f]
GaAs	7.5[a]	8	7.4[b]	7.1[e]	7.8[f]
GaSb	4.5[a]	6	5.6[b]	4.5[e]	5.8[f]
InN	9[a]	10.4	8.2[b]	7.4[e]	7.4[f]
InP	5.4[a]	6	5.1[b]	3.9[e]	3.7[f]
InAs	3.8[a]	3.8	5.7[b]	4.5[e]	3.3[f]
InSb	2.2[a]	4.3	3.6[b]	2.2[e]	2.4[f]
ZnS	1.8[b]	6.8	2.7[b]	2.4[e]	2.4[f]
ZnSe	1.4[b]	5.5	2.6[b]	1.8[e]	2.7[f]
ZnTe	1[b]	4.1	2.3[b]	0.9[e]	2.1[f]
TiC	32[c]	34	18.8[b]	23.9[e]	27[f]
TiN	20.6[c]	21.6	18.7[b]	23.8[h]	23.3[f]
ZrC	25[c]	21	10.7[g]	15.7[h]	27.5[f]

Y. Tian *et al.*, Int. J. Refract. Met. Hard Mater. **33**, 93 (2012).

Crystal	H_{Exp} (GPa)	H_{Tian} (GPa)	$H_{Simunek}$ (GPa)	H_{Xue} (GPa)	H_{Chen} (GPa)
ZrN	15.8[c]	16.7	10.8[g]	15.9[h]	–
HfC	26.1[c]	26.8	10.9[g]	15.6[h]	–
HfN	16.3[c]	18	10.6[g]	15.2[h]	19.2[f]
VC	27.2[c]	23	25.2[g]	17.5[h]	26.2[f]
VN	15.2[c]	14.9	26.5[g]	16.5[h]	–
NbC	17.6[c]	16.1	18.3[b]	12.8[h]	15.4[f]
NbN	13.7[c]	13.6	19.5[b]	12[h]	14.7[f]
TaC	24.5[c]	26	19.9[g]	14.7[h]	–
TaN	22[c]	20	21.2[g]	14.3[h]	–
CrN	11[c]	11	36.6[g]	19.2[h]	–
WC	30[c]	31	21.5[b]	20.6[e]	31.3[f]
Re_2C	17.5[j]	19.7[j]	11.5[g]	16.2[h]	26.4[i]
Al_2O_3	20[c]	18.8	13.5[g]	18.4[h]	20.3[i]
MgO	3.9[d]	4.5	4.4[g]	5.4[h]	24.8[i]
LiF	1[d]	0.8	2.2[g]	–	8.5[i]
NaF	0.6[d]	0.85	1[g]	–	5.7[i]
NaCl	0.2[d]	0.4	0.4[b]	–	2.4[i]
KCl	0.13[d]	0.18	0.2[b]	–	2.3[i]
KBr	0.1[d]	0.23	0.2[g]	–	0.1[i]

[a] Reference [34].
[b] Reference [37].
[c] Reference [32].
[d] Reference [60].
[e] Reference [58].
[f] Reference [30].
[g] Calculated by authors using method [36].
[h] Caculated using [35].
[i] Calculated with [30].
[j] Referenece [52].

One Step Back…
The Mechanism of Hardness

- Intrinsically hard materials are hard because of their short and strong bonds, often covalent in nature.
  - Diamond C (96 GPa), zinc blende BN (63 GPa), zinc blende SiC (31 GPa).
  - Transition metal borides (B), carbides (C), nitrides (N).
  - TiB_2 (25~35 GPa), rocksalt TiC (32 GPa), rocksalt TiN (21 GPa).
  - Nitrides have better oxidation resistance.

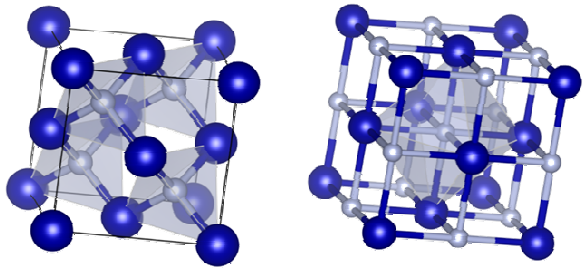

zinc blende *rocksalt*

Gao, He, Wu, Liu, Yu, Li, Phys. Rev. Lett. (2003).
Guo, Li, Liu, Yu, He, Liu, J. Appl. Phys. (2008).
B. Basu et al., International Materials Reviews **51** (2006)

One Step Back…
The Mechanism of Hardness

- Nano-/micro-sized effect induced hardness relies on the nano-/micro-structures to inhibit plastic flow (dislocation progression).
  - Hall-Petch effect $\sigma_C = \sigma_0 + \frac{k_{gb}}{\sqrt{d}}$ is effective down to 10~15 nm. Lower sizes result in grain boundary sliding. It is seen and utilized for a wide range of materials.
  - If there is a way to further lower the grain size while keeping the grain boundaries stable and strong to shear, larger hardness will be achieved.
  - By formation of twin boundaries at nano scale, low energy boundaries. Nano-twinned BN, ~4 nm, 108 GPa.
  - By spinodal decomposition of a solid solution to two phases, with one covering another. nc-TiN/a-Si_3N_4, ~4 nm, 60 GPa.

R. W. Hertzberg, *Deformation and Fracture Mechanics of Engineering Materials*, 3rd ed. Wiley, New York, 1989

Y. Tian et al., Nature **493**, 385 (2013)
S. Veprek, J. Vac. Sci. Technol. A **31** (2013).

One Step Back…
The Mechanism of Hardness

The nano-structures are meant to inhibit the plastic flow, but if the flow is difficult to initiate in the first place, we have more room for nano-sized enhancement.

--- The importance of intrinsic (elastic) properties, which can be done by computations on a large scale.

What can be explored:

- Elastic properties, especially hardness/shear related.
- Their trends and correlation with the electronic structures.
- Thermodynamic stability compared with other competing phases at different temperatures.
- Solid solution elastic properties and thermodynamic stability.

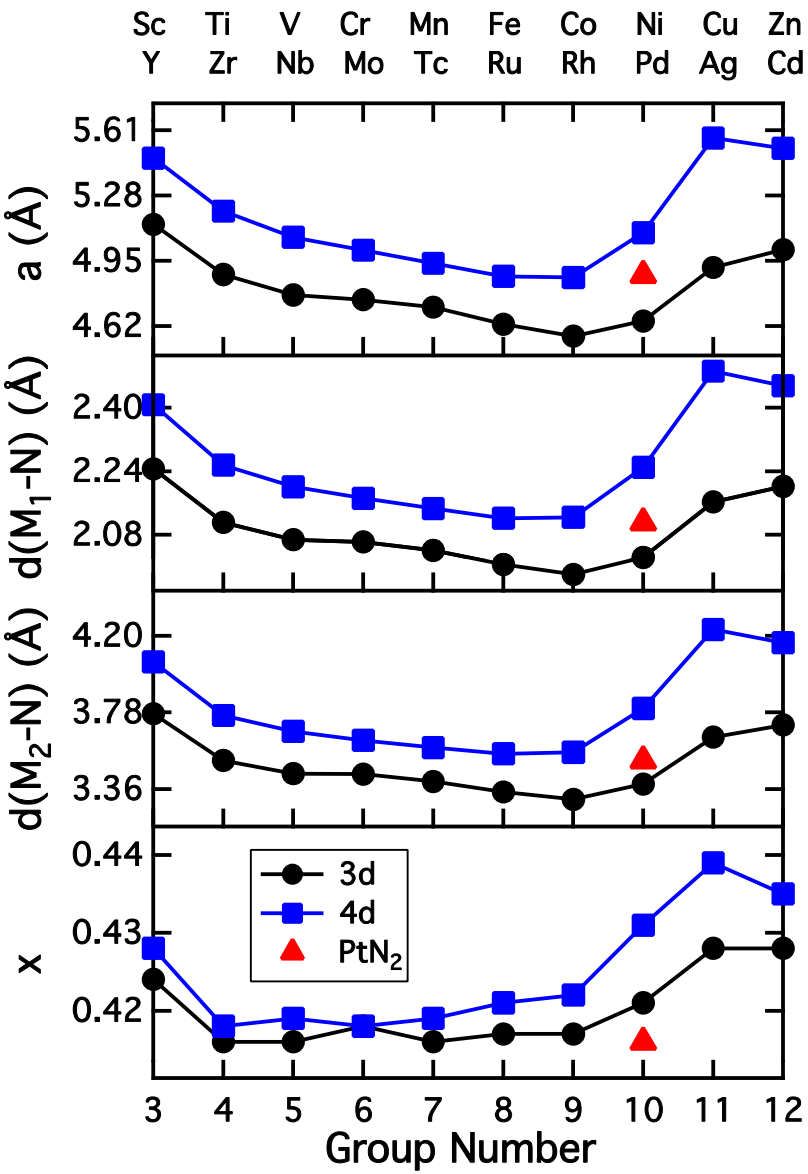

Structural Parameters

Correlations among
a (lattice constant),
$d(M_1\text{-}N)$,
$d(M_2\text{-}N)$,
x (internal parameter of nitrogen)

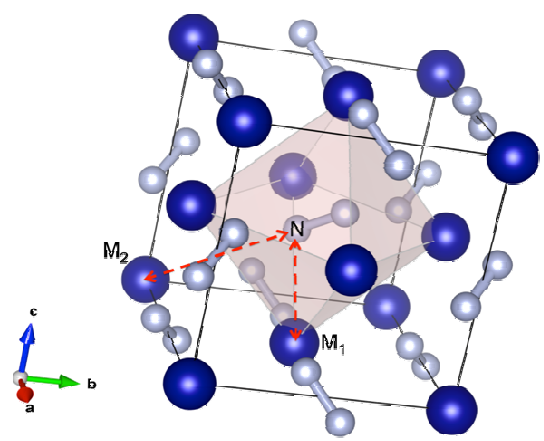

Transition Metal Nitrides

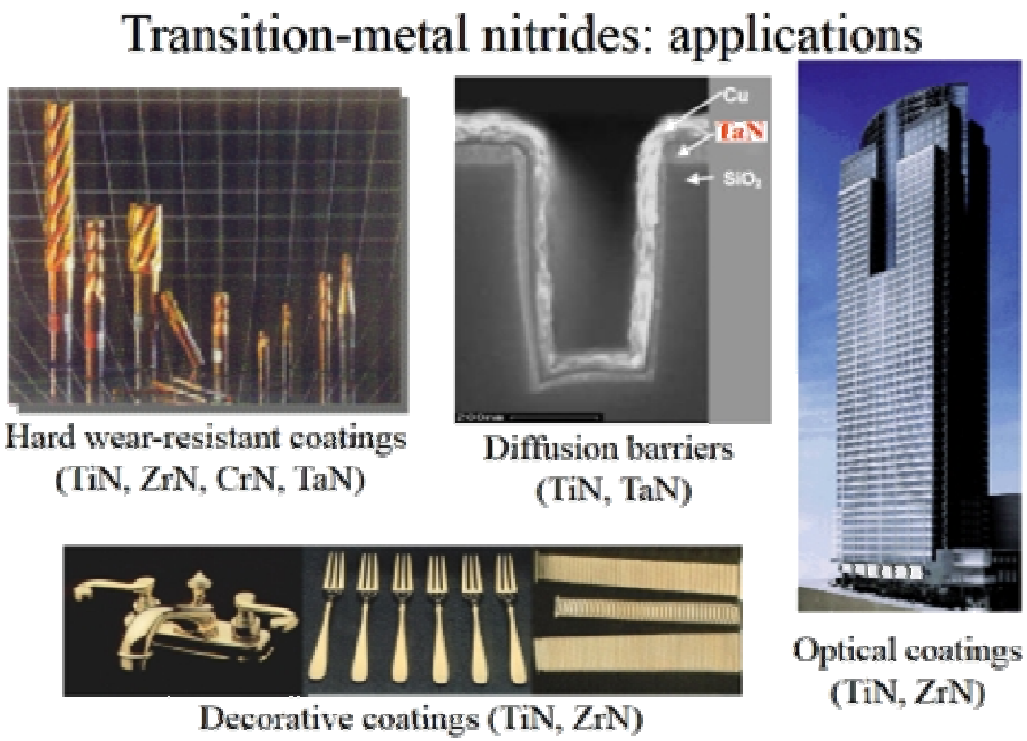

- Wear resistant
- Chemical corrosion/oxidation resistant
- Thermal resistant
- Aesthetically pleasing

Excellent coating materials for multiple purposes

Thermodynamic Stability

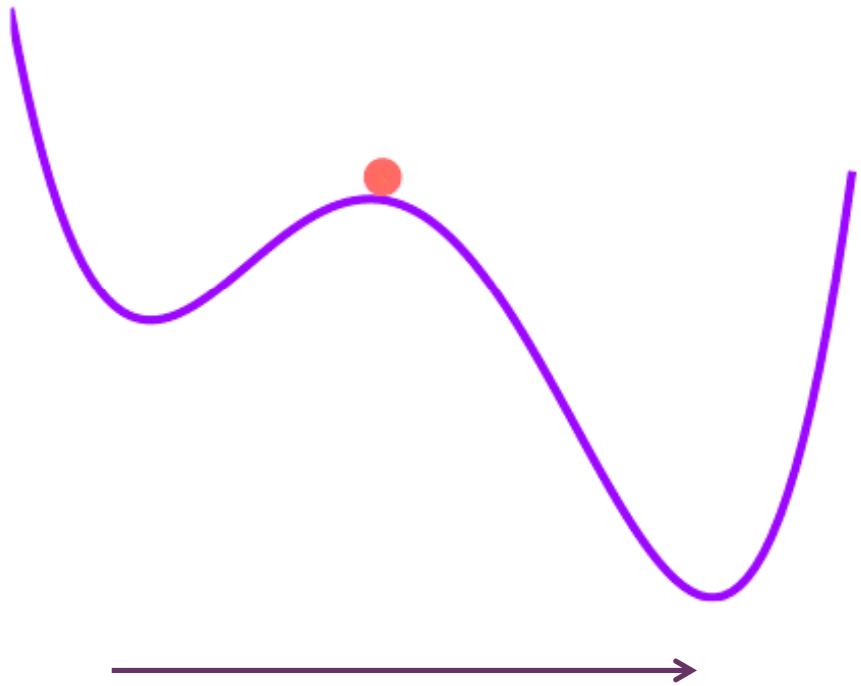

Any kind of transformation, strain, atomic movement.

Comparison with other calculated and experimental values of pyrite-type PtN_2. Mechanically stable pyrite-type 5d phases and fluorite-type 3d and 4d phases are also included. Listed values are equilibrium lattice constant (a), internal parameter (x) of Pa3 Wyckoff position 8c, elastic constants C_{11}, C_{12}, C_{44}, and bulk modulus (B).

	a (Å)	x	C_{11} (GPa)	C_{12} (GPa)	C_{44} (GPa)	B (GPa)
PtN_2 This work	4.877	0.416	661.9	69.3	128.8	266.9
PtN_2 LAPW-GGA [a]	4.862	0.415	668	78	133	272
PtN_2 PP-PW91 [b]	4.877	0.417	713	90	136	298
PtN_2 PP-PBE [c]	4.848	0.415	696	83	136	288
PtN_2 PAW-PW91 [d]	4.875					278
PtN_2, Exp. [e]	4.804					372
pyrite-HfN_2	5.129	0.415	359.4	171.9	124.7	234.4
pyrite-IrN_2	4.858	0.418	691.9	97.8	67.5	295.9

[a] R. Yu, Q. Zhan, and X. F. Zhang, Appl. Phys. Lett. **88**, 051913 (2006).
[b] H. Gou, L. Hou, J. Zhang, G. Sun, L. Gao, and F. Gao, Appl. Phys. Lett. **89**, 141910 (2006).
[c] A. F. Young, J. A. Montoya, C. Sanloup, M. Lazzeri, E. Gregoryanz, and S. Scandolo, Phys. Rev. B **73**, 153102 (2006).
[d] J. C. Crowhurst, A. F. Goncharov, B. Sadigh, C. L. Evans, P. G. Morrall, J. L. Ferreira, and A. J. Nelson, Science **311**, 1275 (2006).
[e] E. Gregoryanz, C. Sanloup, M. Somayazulu, J. Badro, G. Fiquet, H. K. Mao, and R. J. Hemley, Nat. Mater. **3**, 294 (2004).

Inverted integrated projected crystal orbital Hamilton population (−IpCOHP) of the closest M-M, M-N, and N-N bonds of the pyrite-type transition-metal pernitrides, MN_2. Listed are the averaged values of equivalent pairs in a cell. The three columns to the right are the changes in values (δ) when a 10% C_{44} [110]-oriented shearing strain is applied to the conventional unit cell.

Group of M	M of MN_2	Inverted IpCOHP (meV)					
		M-M	M-N	N-N	δ (M-M)	δ (M-N)	δ (N-N)
4	Ti	-2.4	1908.1	5456.0	29.3	-25.9	237.1
	Ti (strained)	26.8	1882.2	5693.1			
5	V	492.8	1654.6	3205.6	42.0	-16.9	45.3
	V (strained)	534.8	1637.7	3250.9			
6	Cr	359.2	1604.4	4051.2	20.6	-12.1	9.3
	Cr (strained)	379.8	1592.2	4060.6			
7	Mn	414.6	1559.8	3502.7	18.6	-11.9	58.2
	Mn (strained)	433.2	1547.8	3560.8			
8	Fe	486.1	1530.1	3730.2	30.2	-9.1	55.5
	Fe (strained)	516.3	1521.0	3785.7			
9	Co	121.7	1802.8	7837.0	25.2	-9.3	69.7
	Co (strained)	146.9	1793.5	7906.7			
10	Ni	82.9	1537.2	8755.5	14.8	-19.4	110.6
	Ni (strained)	97.7	1517.8	8866.0			
12	Zn	-73.3	1095.1	8479.4	9.0	-9.6	65.1
	Zn (strained)	-64.3	1085.5	8544.5			
7 (4d)	Tc	477.4	1754.8	3231.7	48.7	-25.4	195.1
	Tc (strained)	526.1	1729.3	3426.8			
10 (5d)	Pt	-191.3	2391.5	6544.4	-11.2	-23.5	109.6
	Pt (strained)	-202.5	2368.0	6653.9			